Protist, Vol. 170, 233–257, April 2019
http://www.elsevier.de/protis
Published online date 23 March 2019

Protist

ORIGINAL PAPER

Ploeotids Represent Much of the Phylogenetic Diversity of Euglenids

Gordon Lax[a], Won Je Lee[b], Yana Eglit[a], and Alastair Simpson[a,1]

[a]Department of Biology, and Centre for Comparative Genomics and Evolutionary Bioinformatics, Dalhousie University, Halifax, NS, Canada
[b]Department of Environment and Energy Engineering, Kyungnam University, Changwon, Republic of Korea

Submitted November 26, 2018; Accepted March 1, 2019
Monitoring Editor: Julius Lukeš

Ploeotids are an assemblage of rigid phagotrophic euglenids that have 10–12 pellicular strips and glide on their posterior flagellum. Molecular phylogenies place them as a poorly resolved, likely paraphyletic assemblage outside the Spirocuta clade of flexible euglenids, which includes the well-known phototrophs and primary osmotrophs. Here, we report SSU rRNA gene sequences from 38 ploeotids, using both single-cell and culture-based methods. Several contain group I or non-canonical introns. Our phylogenetic analyses place ploeotids in 8 distinct clades: *Olkasia* n. gen., *Hemiolia* n. gen., *Liburna* n. gen., *Lentomonas*, *Decastava*, *Keelungia*, Ploeotiidae, and *Entosiphon*. *Ploeotia vitrea*, the type of *Ploeotia*, is closely related to *P. oblonga* and *Serpenomonas costata*, but not to *Lentomonas*. *Ploeotia* cf. *vitrea* sensu Lax and Simpson 2013 is not related to *P. vitrea* and has a different pellicle strip architecture (as imaged by scanning electron microscopy): it instead represents a novel genus and species, *Olkasia polycarbonata*. We also describe new genera, *Hemiolia* and *Liburna*, for the morphospecies *Anisonema trepidum* and *A. glaciale*. A recent system proposing 13 suprafamilial taxa that include ploeotids is not supported by our phylogenies. The exact relationships between ploeotid groups remain unresolved and multigene phylogenetics or phylogenomics are needed to address this uncertainty.

Key words: Phylogenetics; protist; protozoa; taxonomy; systematics; euglenids.

Introduction

Euglenids (euglenoids) are a diverse group of flagellates distinguished by the euglenid pellicle—a structure underneath the cell membrane that is composed of 4 to >100 abutting proteinaceous strips underlain by microtubules (Leander et al. 2001b). Cells with ≥16 strips are usually flexible, and often capable of dramatic cell-shape changes called 'euglenoid motion' or 'metaboly', while those with 12 or fewer strips are rigid (Leander et al. 2007). Euglenids include organisms with phototrophic, osmotrophic and phagotrophic nutritional modes (Leander et al. 2017). Phagotrophy is the ancestral mode, and some kind of flexible phagotrophic euglenid was likely the host in a secondary endosymbiosis with a member of Pyramimonadales to give rise to phototrophic euglenids (Turmel et al. 2008). This occurred around 600 MYA, according to recent estimates (Jackson et al. 2018).

[1]Corresponding author;
e-mail Alastair.Simpson@Dal.Ca (A. Simpson).

https://doi.org/10.1016/j.protis.2019.03.001

Most phagotrophic euglenids are gliding cells that associate with surfaces. They are found in almost all aquatic habitats (Larsen and Patterson 1990; Lee 2012; Patterson and Simpson 1996; Schroeckh et al. 2003), and in some cases represent the major group of heterotrophic flagellates by biomass (Boenigk and Arndt 2002; Dietrich and Arndt 2000; Lee and Patterson 2002). Phagotrophic euglenids can be crudely divided into three categories: Flexible forms with $\geq$18 strips (e.g. *Peranema, Urceolus, Neometanema, Anisonema*); petalomonads, which are rigid cells, usually with 4–10 strips that glide on their anterior flagellum (e.g. *Petalomonas, Notosolenus, Sphenomonas*); and ploeotids, rigid cells with 10 or 12 strips, which glide on the posterior flagellum (e.g. *Ploeotia, Entosiphon, Keelungia*). The anaerobic symbiontids are sometimes considered phagotrophic euglenids that lack a complete pellicle, but there has not yet been a definitive phylogenetic placement of this group (Adl et al. 2019; Cavalier-Smith 2016; Lax and Simpson 2013; Yubuki et al. 2013).

The phototrophs and osmotrophs are relatively well characterised in terms of phylogenetic relationships and biodiversity. By contrast, our current understanding of phagotrophic euglenid phylogeny and taxonomy is fragmentary, with the major source of phylogenetic knowledge being species-poor SSU-rDNA phylogenies. Numerous analyses have shown that flexible phagotrophic euglenids are closely related to phototrophic and osmotrophic euglenids. This clade of euglenids, characterised by having many helically-arranged strips, was usually referred to as 'H' or 'HP' and recently formalised as 'Spirocuta' or 'Helicales' (Busse et al. 2003; Cavalier-Smith 2016; Lee and Simpson 2014a; Paerschke et al. 2017). Petalomonads and symbiontids are also both apparently monophyletic (Cavalier-Smith et al. 2016; Lax and Simpson 2013). Ploeotids, on the other hand, are invariably not recovered as a clade, instead forming a paraphyletic group that seemingly gave rise to Spirocuta, and possibly petalomonads and/or symbiontids as well (Cavalier-Smith 2016; Chan et al. 2015; Lax and Simpson 2013; Paerschke et al. 2017). This identifies ploeotids as a key assemblage for understanding the early evolutionary history of euglenids.

Ploeotids are 7–60 μm long, often 15–25 μm. They are frequently characterised as bacterivorous (Leander et al. 2001a, 2007; Leander 2004), though there are some reports of ingested eukaryote cells (e.g. Lax and Simpson 2013; Linton and Triemer 1999). Cells glide on the thickened, sometimes very long, posterior flagellum. Many cells also exhibit a 'jerking back' motion with their posterior flagellum, similar to the spirocute *Anisonema* (e.g. Al-Qassab et al. 2002). The anterior flagellum is directed forward and either sweeps from side to side or is just held in front, and likely is used to detect prey. Ploeotids (see below for taxonomy) are mostly found in marine environments and almost always have 10 pellicle strips, though the arrangement and fine structure of strips differs considerably. For example, *Ploeotia vitrea* has 10 similar strips that meet at sharp keels, whereas *Serpenomonas/Ploeotia costata* has 5 broad strips alternating with 5 very narrow strips that lie within grooves. *Lentomonas* has 7 humped strips that feature prominently on the dorsal side, while the three ventral strips are flat. *Keelungia* and *Decastava* both have 10 similar relatively flat strips around the cell body (Cavalier-Smith et al. 2016; Chan et al. 2013). *Entosiphon* is unusual in often or always having 12 pellicular strips that mostly alternate in form (Larsen and Patterson 1990; Triemer and Fritz 1987).

The genus *Ploeotia* itself was introduced in 1841 when Dujardin described *Ploeotia vitrea* (Dujardin 1841), but was then mostly forgotten until the mid 1980s. Over the next two decades the genus was 'redescribed' by Farmer and Triemer (1988) using transmission and scanning electron microscopy data, and $\sim$20 additional species were described via light microscopy (e.g. Al-Qassab et al. 2002; Larsen and Patterson 1990; Patterson and Simpson 1996). Over the same time, two additional genera were introduced based on light- and electron microscopy data. *Serpenomonas* (type species *Serpenomonas costata*) was established as a genus without considering *Ploeotia* (Triemer 1986) and was shortly after merged with *Ploeotia* (Farmer and Triemer 1988). *Lentomonas* was discriminated from *Ploeotia* on the basis of ultrastructural data (Farmer and Triemer 1994), which came from an organism indistinguishable from *Ploeotia corrugata*, described slightly earlier (Larsen and Patterson 1990). Consequently, *Lentomonas* was often also treated as a junior synonym of *Ploeotia* (Ekebom et al. 1995; Patterson and Simpson 1996), leading to a 'lumping' situation where all ploeotids other than *Entosiphon* were assigned to a single genus. Prior to 2013 the only molecular data available for ploeotids was from *Ploeotia/Serpenomonas costata*, and from *Entosiphon* strains with extremely rapidly evolving SSU-rRNA genes (Paerschke et al. 2017; von der Heyden et al. 2004). Recent phylogenies that include a couple of additional species

have shown the ploeotids to be divergent one from other (Cavalier-Smith et al. 2016; Chan et al. 2013; Lax and Simpson 2013). This has led to taxonomic 'splitting' at the genus level, including the description of two new genera, *Keelungia* and *Decastava* (Cavalier-Smith et al. 2016; Chan et al. 2013), and moves to again recognise *Serpenomonas* and *Lentomonas* as distinct from *Ploeotia* (Cavalier-Smith 2016). Cavalier-Smith (2016) has further proposed a highly detailed assignment of ploeotid genera into families, orders, subclasses, classes and superclasses. Nonetheless, prior to our study, SSU-rRNA genes were available for only four nominal ploeotid species outside of *Entosiphon*: *Ploeotia/Serpenomonas costata* (Busse and Preisfeld 2003; Chan et al. 2015), *Keelungia pulex* (Chan et al. 2013), *Decastava edaphica* (Cavalier-Smith et al. 2016; Paerschke et al. 2017; the sequences reported under the names *Decastava edaphica* and *Ploeotia edaphica* are derived from the same culture and are 99.3% identical) and a cell identified as *Ploeotia* cf. *vitrea* (Lax and Simpson 2013), plus HSP90 sequences from just three species (Breglia et al. 2007; Cavalier-Smith et al. 2016). Crucially, the type species of *Ploeotia*, *P. vitrea*, has never been examined using molecular methods. It was recently assumed that its placement was to follow *Ploeotia* cf. *vitrea* (Cavalier-Smith et al. 2016), notwithstanding an explicit caveat that this would require confirmation (Lax and Simpson 2013). In fact, this assumption was used to justify placement of *P. vitrea* and *S./P. costata* in separate classes within the taxonomy discussed above (Cavalier-Smith et al. 2016; Cavalier-Smith 2016). There has not been any molecular data for *Lentomonas*.

Considering the genus *Anisonema* adds an additional complication. *Anisonema* currently includes the type species, *Anisonema acinus*, and ~20 other nominal species. Many of these are similar to ploeotids in the arrangement of their flagella. As with several other phagotrophic euglenid genera, it is unclear how many of these morphospecies actually belong to *Anisonema*, since the genus assignments are partly based on questionable morphological characters, such as the visibility of the feeding apparatus with light microscopy (Larsen and Patterson 1990). The only molecular data available up to now has been SSU rRNA gene sequences from several *A. acinus* (-like) populations/cells, which prove to belong to Spirocuta (Busse et al. 2003; Lax and Simpson 2013). Unfortunately, the absence of sequence data from other morphotypes has made it impossible to test whether all nominal *Anisonema* species belong to Spirocuta. Notably, the morphotypes *A. trepidum* and *A. glaciale* have not been reported to show flexibility, and both differ noticeably from *A. acinus* in their locomotion and flagellar movement patterns (Larsen 1987; Larsen and Patterson 1990).

This study aims to examine the broad-scale molecular diversity of ploeotids, to better understand their phylogenetic affinities and clarify their systematics. We established 10 cultures representing the morphospecies *Ploeotia vitrea, Ploeotia/Serpenomonas costata, Ploeotia oblonga,* and *Keelungia* sp. We also derived SSU-rRNA gene sequences from 27 photodocumented single cells, including *Lentomonas* morphotypes, as well as cells identified morphologically as *Anisonema glaciale* and *A. trepidum*. Phylogenetic analyses show that ploeotids sensu lato (i.e. including *Entosiphon* as well as *Ploeotia*-like anisonemids) represent at least 8 major molecular lineages. Crucially, *P. vitrea* is not specifically related to *P.* cf. *vitrea* sensu Lax and Simpson (2013), and instead is closely and robustly related to *S./P. costata* (and *P. oblonga*). This refutes the notion that *Serpenomonas* and *Ploeotia* should belong to different high-rank taxa. We show by SEM that the pellicle structure of *Ploeotia* cf. *vitrea* is distinctly different from *Ploeotia vitrea*, and based on the combined molecular and morphological data propose a new genus and species, *Olkasia polycarbonata* n. gen. n. sp., for *Ploeotia* cf. *vitrea* sensu Lax and Simpson (2013). *Anisonema trepidum* and *A. glaciale*-like cells clearly branch outside of Spirocuta—since they are phylogenetically distinct from the genus *Anisonema*, we propose the new genus *Hemiolia* n. gen. for *Anisonema trepidum* Larsen, 1987; and *Liburna* n. gen. for *Anisonema glaciale* Larsen and Patterson, 1990

Results

Studied Isolates

The organism codes, the assigned taxa and GenBank accession codes for all studied cultures/cells can be found in Table A1 (Supplementary Material).

Ploeotia vitrea

Three cultures of *Ploeotia vitrea* were established, with an additional single cell isolated from a sediment sample (isolate STS2, Supplementary Material Table A1). Cells are oval, with a pointed posterior end and a conspicuous hook-shaped feeding apparatus that extends almost down the complete length of the cell (Figs 1a–b,

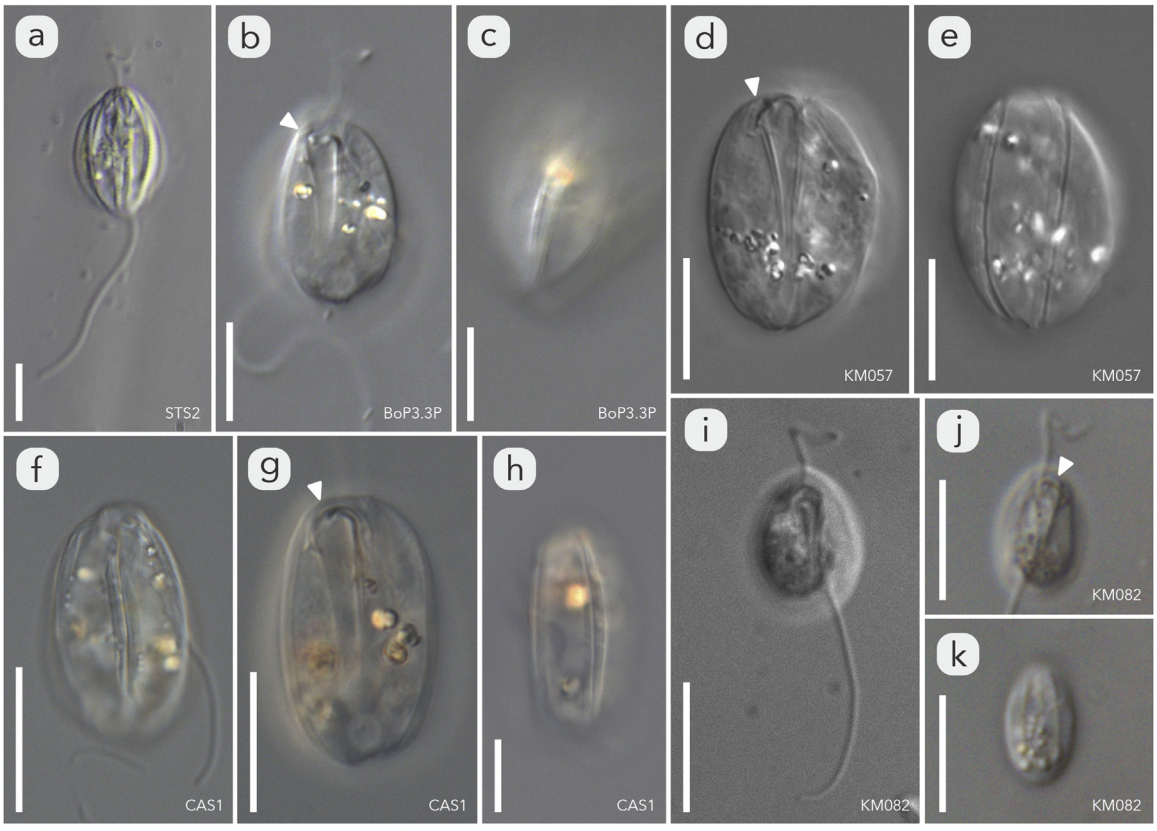

Figure 1. Light micrographs of ploeotid taxa derived from cultures and single cells. (a–c) *Ploeotia vitrea*. (c) shows pellicle strip arrangement at posterior end. (d–e) *Serpenomonas costata*. Note undulating edges of pellicle strips in (e). (f–h) *Ploeotia oblonga*. Pigmented ingesta are ~1.5 μm in diameter. (i–k) *Keelungia* sp. strain KM082. Arrowheads in all images show feeding apparatuses. Scale bars are 10 μm. Isolate names are shown in image. All images were acquired with differential interference contrast optics.

Table 1. Morphological measurements of ploeotid cultures, with mean length and width (including standard deviations), and mean relative anterior and posterior flagellum lengths, derived from 30 cells each.

Species	Strain	Length	Width	Ant. flagellum	Post. flagellum
Ploeotia vitrea	BoP3.3P1[a]	17.5–24.9 μm	11.8–14.1 μm	0.6X	2.65X
	SJB2	18.3 μm (±1.7)	12.5 μm (±2.1)	0.8X	2.75X
	MX-CHA	20.4 μm (±1.6)	14.6 μm (±1.9)	0.7X	2.25X
Ploeotia oblonga	CAS1	20.4 μm (±2.2)	14.6 μm (±2.1)	0.7X	2.3X
Serpenomonas costata	BOP4.1N3	18.4 μm (±1.1)	10.9 μm (±1)	0.7X	2X
	HAK-MF	19.2 μm (±2)	12 μm (±1.7)	0.7X	2.1X
	KM040	19.3 μm (±0.8)	11.1 μm (±0.9)	0.7X	2.4X
	KM057	20.6 μm (±1.2)	14.3 μm (±1.3)	0.7X	1.6X
Keelungia sp.	KM082	10.7 μm (±0.8)	6.7 μm (±0.8)	1.25X	3X
Entosiphon sp.	ESC[b]	21.2 μm (±1.7)	10.1 μm (±1.4)	1X	2.9X

[a]Measurements for BoP3.3P are based on only 2 cells, since the culture was lost before more measurements could be taken.
[b]Measurement for ESC are based on nine cells.

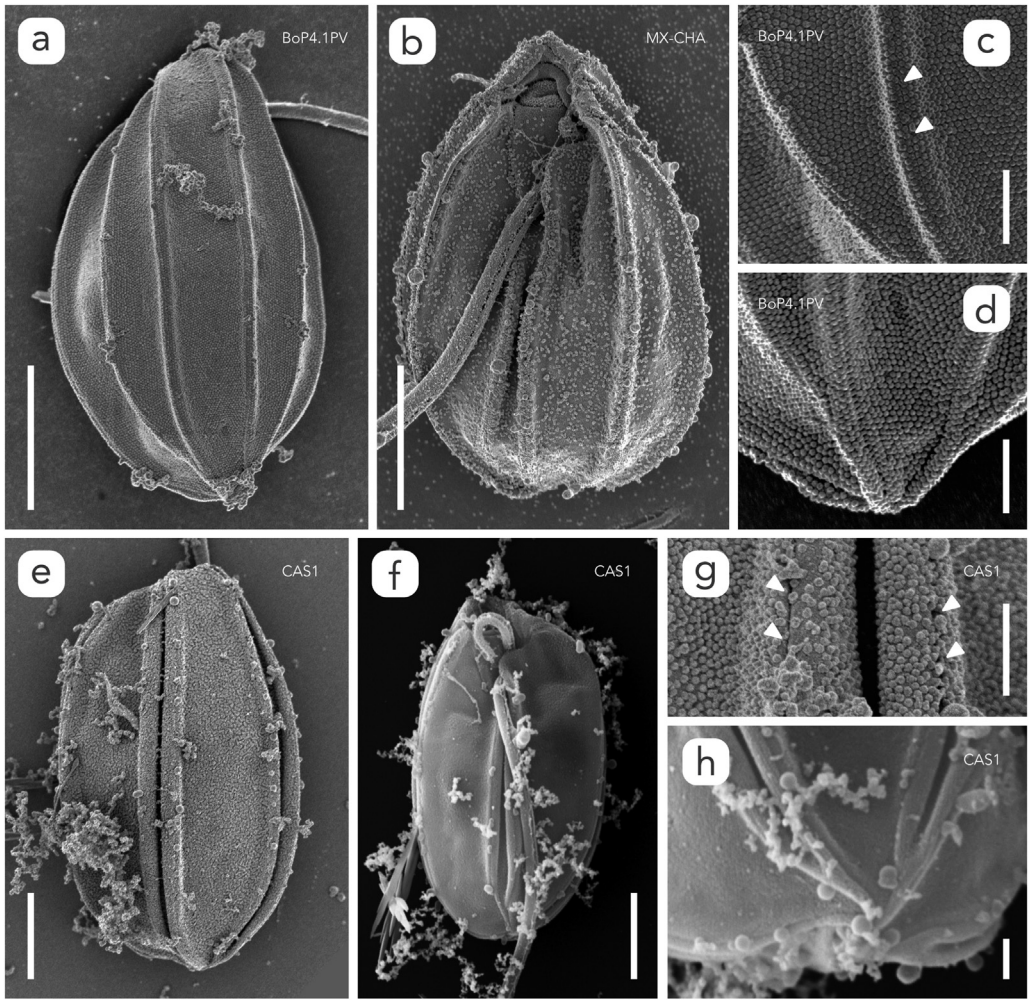

Figure 2. Scanning electron microscopy images of *Ploeotia vitrea* and *Ploeotia oblonga*. (a–d) *Ploeotia vitrea* strains BoP4.1PV (a, c, d) and MX-CHA (b), showing the dorsal (a) and ventral sides (b). The pellicle strip boundaries raised on keels are shown in (c) and at the posterior end in (d). (e–h) *Ploeotia oblonga* strain CAS1, with the dorsal (e) and ventral (f) sides shown. Details of the pellicle strip arrangement are shown in (g) and the posterior end in (h). Arrowheads denote joints between two pellicle strips. Scale bars are 5 μm for (a–b) and (e–f), and 1 μm for (c–d) and (g–h).

2a). The 10 pellicle strips are roughly evenly spaced and raised at their edges to form characteristic keels, or 'double-raised ridges', that are readily visible with light microscopy when viewed in grazing optical section or cross-section (Fig. 1c). SEM confirms that the small grooves at the connections between strips run along the spines of these keels (Fig. 2a–d). The central ventral strip is narrower than other strips (Fig. 2b). Every second strip is slightly shorter than the adjacent strips, such that the keels of the strips come together in a 5-point star at the posterior end of the cell (Fig. 2a, d). Movement is typical of ploeotids: cells glide with their posterior flagellum attached to the surface and trailing behind, whereas the anterior flagellum sweeps from side to side in front of the cell (see Supplementary Material Video 1). Feeding on bacteria was observed in cultures: if the anterior flagellum encounters a suitable prey, the whole cell pulls close to it with the anterior flagellum attached to the bacterium. The *P. vitrea* cell then tips itself over its prey. Measurements of cultured cells are listed in Table 1. In addition to bacteria, culture MX-CHA was tested and found to be able to grow on *Phaeodactylum* sp. (a pennate diatom), in which case cells often contained pigmented ingesta 3.7–6.7 μm in diameter (n = 31), and some cells contained whole diatoms (20.5–25.9 μm long, 4.1–4.2 μm wide; n = 3).

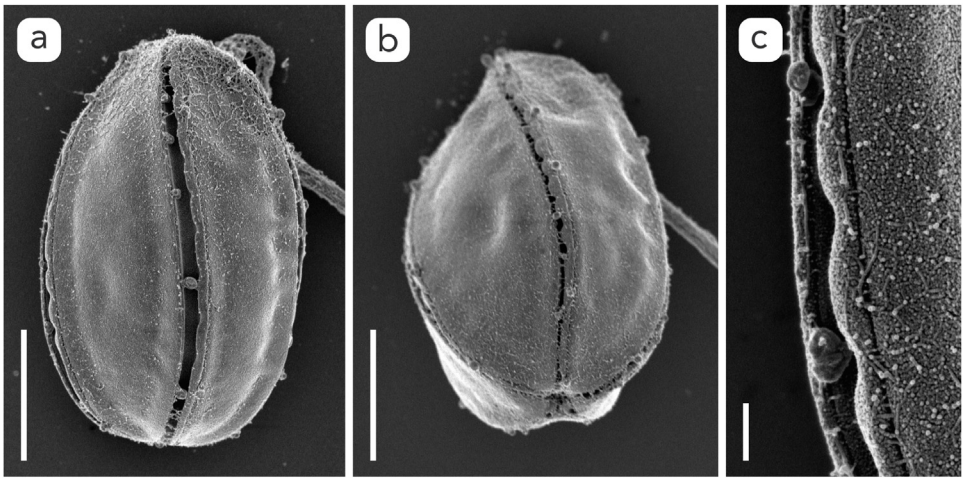

Figure 3. Scanning electron microscopy images of *Serpenomonas costata* strain HAK-MF. (a) dorsal side with pellicle strips clearly visible. (b) dorsal posterior, with star-shaped pellicle arrangement. (c) joint between a wide and narrow pellicle strip. Note the characteristic undulating edge within the narrow strip. Scale bars are 5 μm for (a–b), and 1 μm for (c).

Ploeotia oblonga

We established one culture of *Ploeotia oblonga*, strain CAS1. Cells are oblong, with the hook-shaped feeding apparatus extending down almost the full length of the cell (Fig. 1f–g). The 10 pellicle strips are parallel to the cell outline, but as in *Serpenomonas costata* (see below), alternate between narrow and broad strips (Figs 1f, h, 2e), with the central-most ventral strip being narrow (Fig. 2f). In SEM, the fine structure of the pellicle is revealed to be similar to *P. vitrea* in having the boundaries between adjacent strips raised on keels, though these are lower and broader than in *P. vitrea* (Fig. 2g). The keels come together in a 5-pronged star-shaped pattern at the posterior end of the cell, similar to *P. vitrea* (Fig. 2h). Movement of cells is similar to *P. vitrea* and *S. costata* (Supplementary Material Videos 1 and 2). Cells of CAS1 are capable of ingesting a coccoid alga ~1.5 μm across (bright inclusions in Fig. 1f–h). Morphological measurements are listed in Table 1.

Serpenomonas costata (Ploeotia costata)

We established four cultures of *Serpenomonas costata*, and isolated one cell from a sample (isolate ABF1). Cells are oval and have a conspicuous hook-shaped feeding apparatus (Fig. 1d). The 10 pellicle strips alternate in size, such that cells appear to only have 5 strips separated by deep grooves when viewed with light microscopy (Fig. 1e), but each groove actually houses most of another narrow pellicle strip, as shown by SEM (Fig. 3a–c). Characteristically, SEM shows that the visible part of each narrow strip has an undulating edge that extends over the groove (Fig. 3c). Movement of cells is very similar to that of *Ploeotia vitrea* (Supplementary Material Video 2). Feeding on bacteria was observed in culture and was the same as in *P. vitrea* (see above). Measurements of individual cultures are listed in Table 1. In addition to bacteria, strain KM040 was tested and found to be able to grow on *Phaeodactylum* sp., with most cells containing pigmented ingesta 3.5–6.6 μm in diameter (n = 16). A few cells (all moribund at time of observation) contained whole diatoms (21.1–33.6 μm long, 3.9–7.6 μm wide; n = 3). Sequence identity within clade A (see below; without intron sequences) is 97–99.4%, and is 98–99.5% within clade B. Sequence identity between members of clades A and B is 73.3–75.8% (Supplementary Material Table A3).

Keelungia sp. KM082

We established a culture of *Keelungia* sp. (strain KM082) and sequenced its full-length SSU-rRNA gene. Cells are oblong to ovoid in profile, not flattened, and 9–13 μm long and 4.6–8 μm wide (Fig. 1i). The hook-shaped feeding apparatus is conspicuous, broad on the anterior end and tapers considerably while extending ¾ or more down the cell (Fig. 1i, j). The anterior flagellum is about 1.25X cell length, whereas the thicker (but tapering towards the distal end) posterior flagellum is 3X cell length and trails behind (Fig. 1i). Three faint pellicle strip joints can be seen on both the ventral and the dorsal side, with four laterally (total 10;

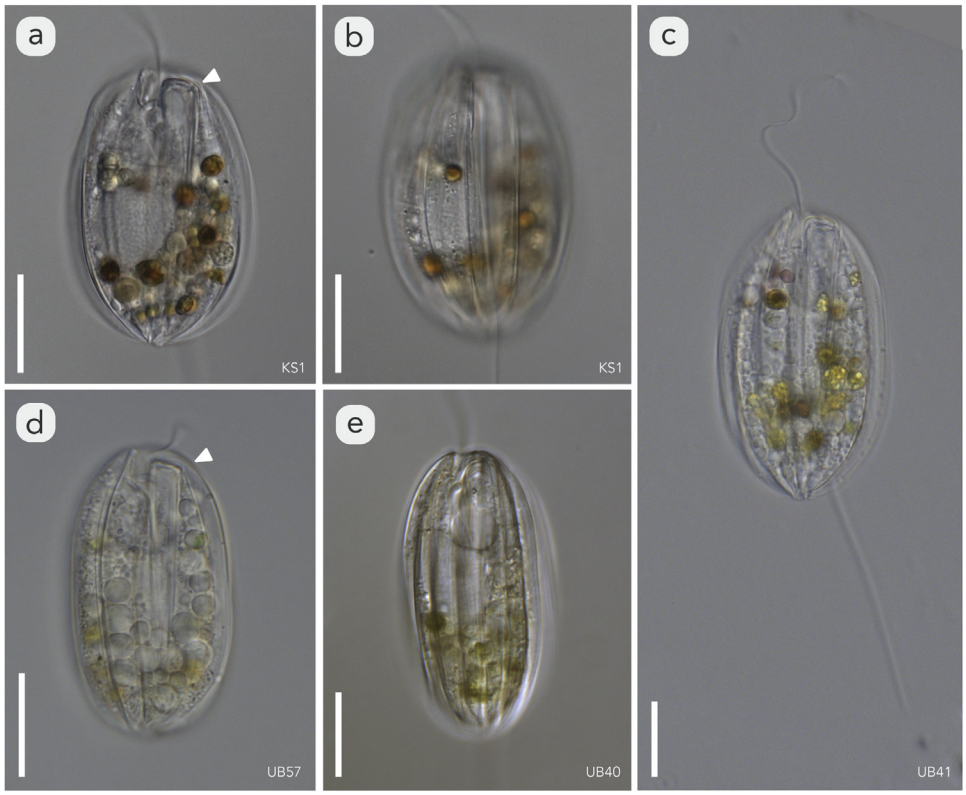

Figure 4. Light micrographs of *Olkasia polycarbonata* n. gen. n. sp., with strain names in image. (a–c) Cells from clade A, with pigmented ingesta 1.2–5.2 μm in diameter; (d–e) Cells from clade B. Arrowheads show feeding apparatus. All scale bars are 20 μm, all images were acquired with differential interference contrast optics.

Fig. 1k). When tested, KM082 was able to feed on *Phaeodactylum* sp. material, with cells containing 2 to more than 10 small pigmented ingesta (1–2.9 μm in diameter; n = 5). Morphological measurements can be found in Table 1.

Olkasia polycarbonata n. gen. n. sp.

We generated SSU-rDNA data for six isolated cells from two different locations. Additionally, we used SEM to image cells that were isolated at the same times as two cells that were processed for sequencing, namely UB41 and UB58 (see Methods). Cells studied by light microscopy are oblong, 55–62.8 μm long by 30.4–37.2 μm wide, ventrally flattened, and have a conspicuous chisel-shaped feeding apparatus that extends down the whole length of the cell (Figs 4a, c–d and 5a–d; morphological measurements of the six cells isolated for molecular work are listed in Supplementary Material Table A2). With SEM, the anterior end of the feeding apparatus can be seen ventrally, and appears 'capped' (Fig. 5d, e). The pellicle is composed of 10 roughly equal-size strips that can be clearly seen with light microscopy (Fig. 4b–c, e). With SEM, the strips appear as S-shaped in cross-section (especially on the dorsal side; Fig. 5a) and overlapping with each other, such that the joints between strips face laterally, rather than running along the spine of each ridge as in *P. vitrea* (Fig. 5b). The posterior flagellum is 1.8X cell length, and conspicuously thickened. Cell movement is similar to that of most other ploeotids: Cells move their anterior flagellum (0.9X cell length) with a sweeping motion, and jerk back when under duress (Supplementary Material Video 3). Structures resembling discharged extrusomes with diameter ~100 nm were observed in some SEM preparations (Fig. 5f). Efforts to establish cultures were unsuccessful. Most observed cells contained algal material in the form of rounded ingesta 2.1–3.6 μm in diameter (Fig. 4a–c). Sequences in clade A (see below) are 97.7–99.8% identical to each other, whereas in clade B 97.8% of sites are identical. Sequence identity between clade A and B is 90.6–93.5% (Supplementary Material Table A3).

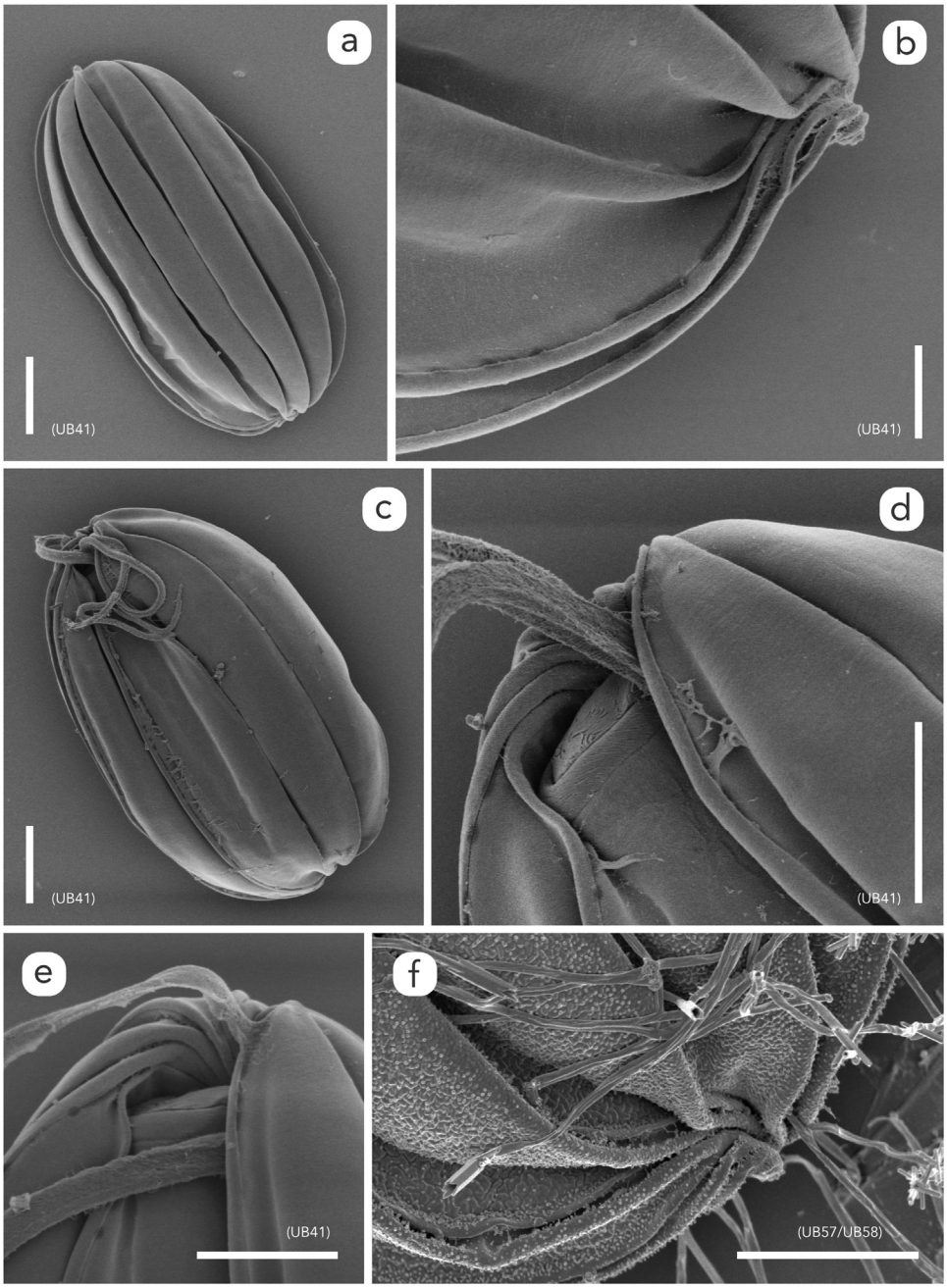

Figure 5. Scanning electron microscopy images of single cells of *Olkasia polycarbonata* n. gen. n. sp. Cells in (a–e) were isolated from the same population as UB41 in clade A; Cell in (f) was isolated from same population as UB57 and UB58 in clade B. (a) dorsal side showing overall pellicle arrangement. (b) detail of posterior dorsal end of a different cell, showing pellicle strip joints. (c) ventral side. (d) detail of ventral anterior, showing feeding apparatus. (e) detail of ventral anterior pellicle strip joints. (f) close-up of dorsal posterior, showing discharging extrusomes. Scale bars are 10 μm for (a and c), 5 μm for (d– f), 2 μm for (b). (a–e) are images of part of the hapantotype of *Olkasia polycarbonata*.

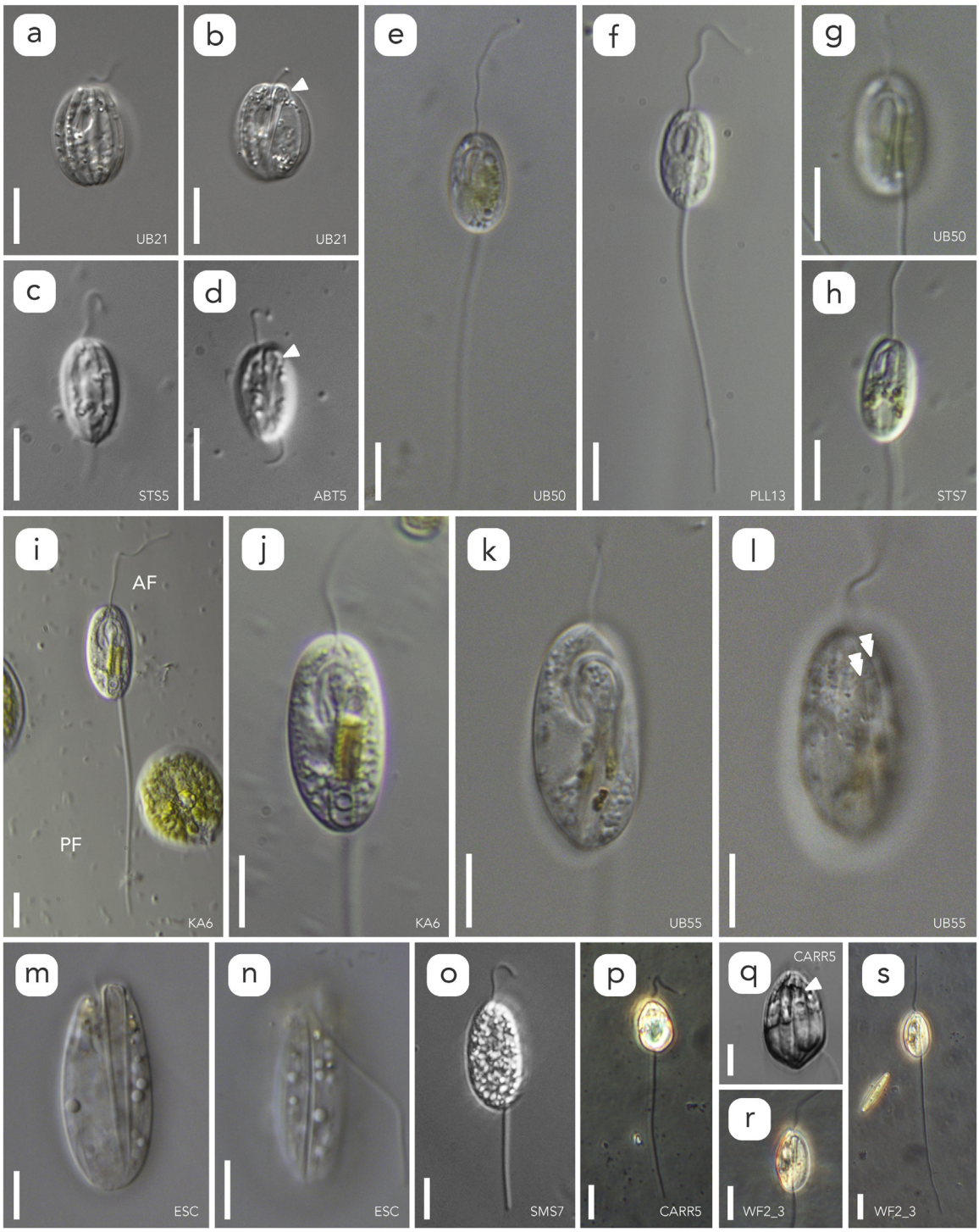

Figure 6. Light micrographs of ploeotid single cell isolates and cultures. (a–b) *Lentomonas corrugata* isolate UB21, showing the dorsal corrugated appearance (a) and arrowhead pointing to feeding apparatus (b). c–d) *Lentomonas azurina*, general view and dorsal side in (c) (isolate STS5), arrowhead pointing to feeding apparatus in (d) (isolate ABT5, no molecular data). (e–h) *Hemiolia trepidum* n. gen n. comb., several isolates. General appearance in isolate UB50 (e) and PLL13 (f), with details of the proximal posterior flagellum in UB50 (g), and pellicle striation in STS7 (h). Note the 10.3 $\times$ 4.3 μm ingested diatom in (e). i–l) *Liburna glaciale* n. gen n. comb., several isolates. General view of isolate KA6 (i), and detail of cell body with flagellar pocket and 19.6 $\times$ 4.3 μm

Lentomonas azurina and *Lentomonas corrugata*

We generated SSU-rRNA gene sequence data from four isolated single cells belonging to the morphospecies *L. corrugata* and one from *L. azurina* (Cell STS5). Both morphospecies are elliptical in profile, ventrally flattened and dorsally convex (Fig. 6a, c). The ratio of length/width for *L. corrugata* cells is 1.14–1.36 (average 1.24), whereas it is 1.73–1.89 (average 1.78) for cells identified as L. azurina (STS5 and two cells for which no molecular data could be acquired; see Supplementary Material Table A2). The dorsal side shows seven strongly corrugated pellicle strips, including two lateral ones (Fig. 6a, c), while the ventral side has three flatter strips (total 10). The feeding apparatus is hook-shaped, oblique, and extends to almost the full length of the cell (Fig. 6b, d). Cells pull back frequently during gliding (Video 4). 97.2–99.8% of sites are identical between *L. corrugata* and *L. azurina* STS5, while there is 95–99.8% identity amongst different *L. corrugata* cells (Supplementary Material Table A3).

Hemiolia trepidum n. gen. n. comb.

We generated SSU-rDNA sequences from six cells identified morphologically as *Anisonema trepidum* (Larsen 1987). This morphotype has an oblong cell shape and is moderately flattened (Fig. 6e–h). Three to four faint pellicle striations are sometimes seen on the dorsal side (Fig. 6h). Cells glide rapidly in relatively straight lines, often with occasional stops when cells sit with only the anterior flagellum beating for 1–2 s, and then resume movement in the same direction. Characteristically, the anterior flagellum is held to the right-hand side of the cell, performing a trembling motion with the distal quarter of the flagellum. The 'jerking-back' motion that is common in *Anisonema acinus* is less frequent and is always followed by an abrupt change in direction (Supplementary Material Video 5). Lengths for the 4 cells observed were 12.4–22.7 μm (average 16.8 μm), and widths 7.3–9.9 μm (average 8.5 μm). Anterior flagella were typically 1.5X cell length, and posterior flagella were 3.3X cell length. The feeding apparatus could not be observed by light microscopy. Three of the isolated cells had ingested whole diatoms (e.g. Fig. 6e; ingested cell is 10.3 × 4.3 μm). Individual measurements of single cells are listed in Supplementary Material Table A2.

Liburna glaciale n. gen. n. comb.

SSU-rDNA sequences were generated from five cells identified as *Anisonema glaciale* (Larsen and Patterson 1990). Like *Hemiolia trepidum*, these cells have an oblong cell shape and are moderately flattened (Fig. 6i–l), but are substantially larger in size, averaging 26.1 μm in length (25.4–27.1 μm), and 12.4 μm in width (11.4–13.9 μm). Dorsally, 5–6 faint pellicle striations were sometimes observed (Fig. 6l). Like *Hemiolia trepidum*, *Liburna* exhibits the movement pattern of gliding rapidly in straight lines, with the anterior flagellum held to the right side (Supplementary Material Video 6). The anterior flagellum is approximately 1.4X cell length, while the posterior flagellum is ∼3X cell length. A feeding apparatus was not observed by light microscopy. Three out of five cells isolated had ingested whole diatoms (Fig. 6i–k; two were measurable: 19.6 × 4.3 μm and 17 × 4 μm). Measurements of single cells can be found in Supplementary Material Table A2.

Entosiphon sp. ESC

A partial SSU-rRNA sequence of *Entosiphon* sp. strain ESC was acquired through transcriptome sequencing that will be reported elsewhere (Lax et al. unpublished). Cells are oblong and elongated, with a conspicuous moving feeding apparatus with strong rods, extending down the whole length of the cell (Fig. 6m). 12 clearly visible pellicle strips run straight down the length of the cell. Narrower pellicle strips alternate with broader strips, at least on the dorsal side (Fig. 6n). Strain ESC feeds on material from *Haematococcus* sp. in culture (see bright inclusions at anterior in Fig. 6m). Morphological measurements can be found in Table 1.

ingested diatom visible (j). Detail of flagellar pocket in isolate UB55 and 17 × 4 μm ingested diatom (k) and pellicle striations (arrowheads) in (l). m–n) *Entosiphon* sp. strain ESC, chisel-shaped feeding apparatus in m), and pellicle striations in n). (o) Unidentified ploeotid isolate SMS7, general appearance. The posterior flagellum of this cell was truncated at time of imaging. (p–q) Isolate CARR5, general appearance (p) and close-up of pellicle striations (q) (arrowhead). (r–s) Isolate WF2_3, close-up of cell body (r) and general appearance (s). All scale bars are 10 μm. Images were acquired with differential interference contrast optics, except for (p, r, s) where phase contrast optics were used.

Unidentified ploeotid SMS7

A partial SSU-rDNA was sequenced. The $16.2 \times 8.2\,\mu m$ cell is oblong and covered in refractile granules (Fig. 6o), making observation of internal or pellicle structures impossible with available optics. The cell glides on the thick posterior flagellum (5X cell length). Beating of the thick anterior flagellum (~1.5X cell length) during movement was similar to *Liburna* and *Hemiolia*, but more active and in a broader arc.

Unidentified ploeotid CARR5

A partial SSU-rDNA was sequenced. The $31.9 \times 20\,\mu m$ cell is roughly pyriform, with a pointed posterior end (Fig. 6p, q). The anterior flagellum appears thick (~1X cell length), whereas the very thick posterior flagellum (4.5X cell length) tapers slightly. Four strongly developed pellicle strip joints can be seen on the dorsal, and four on the ventral side (Fig. 6q, number of lateral strips unclear).

Unidentified ploeotid WF2_3

A partial SSU-rDNA was sequenced. The $36.2 \times 20.6\,\mu m$ cell is oblong (Fig. 6r, s) and glides on a thickened, tapering posterior flagellum (5X cell length; Fig. 6s). The anterior flagellum (~1X cell length) is held on one side like in *Hemiolia*. The ingestion organelle extends down half the cell length (Fig. 6r). Since this cell was only imaged using phase contrast optics, no pellicle strip joints could be seen.

Phylogeny

We conducted six separate phylogenetic analyses, differing in taxon sampling: (1) No *Entosiphon*, no outgroup (main dataset); (2) No *Entosiphon*, with outgroup; (3) With *Entosiphon*, no outgroup; (4) With *Entosiphon*, with outgroups; (5) No *Entosiphon*, with outgroups, no partial sequences (<1000 bp, 9 sequences excluded); (6) No *Entosiphon*, no outgroup, and no 'rogue taxa' (see Methods). All datasets were subjected to Maximum Likelihood (ML) analyses under the GTR + Γ model, with robustness estimated from 1000 bootstrap replicates. Datasets 1 and 3 were also subjected to a Bayesian analysis under the same model (see Methods for further details).

The Euglenida (with symbiontids) grouping consists of several well-supported clades, with little robust phylogenetic structure linking them. These are: (a) The clade Spirocuta, containing phototrophic euglenids (Euglenophyceae), primary osmotrophic euglenids (Aphagea) and phagotrophic euglenids with a flexible pellicle (Supplementary Material Table A4); (b) Petalomonadida (fully supported in all analyses); (c) Symbiontida (fully supported in all analyses); and (d) eight clades of ploeotid sequences, as described below (Figs 7, 8).

The new genus *Olkasia* is represented by *Olkasia polycarbonata* n. sp. (=*Ploeotia* cf. *vitrea* sensu Lax and Simpson, 2013). In all analyses, six novel sequences branched with maximum support with the one previously reported sequence (Lax and Simpson 2013). Two strongly supported subgroups were recovered within this clade (clade A and clade B, 95–100% BS, 1 pp). In four out of the five datasets that included unidentified ploeotid SMS7, it branched sister to *Olkasia*, although with negligible support (25–41% BS and 0.55 pp; Figs 7, 8). The novel genus *Hemiolia* includes six cells identified as *H. trepidum* (basionym *Anisonema trepidum*), always on a long and maximally supported branch (Fig. 7). The partial sequence of unidentified ploeotid WF2_3 branched as sister to this clade in three of the four analyses where it was included, but with negligible support (e.g. Fig. 7). Novel genus *Liburna* was composed of five cells identified as *L. glaciale* (basionym *Anisonema glaciale*), always forming a maximally supported clade. Branch lengths between individual sequences were short. The partial sequence of unidentified ploeotid CARR5 fell sister to the *Liburna* clade in five out of the six analyses when it was included, albeit with poor-to-no support (19–47% BS; e.g. Fig. 7). *Lentomonas* included four novel sequences of *L. corrugata* and one sequence of *L. azurina*, forming a clade with maximum support in both ML and Bayesian analyses. The *L. azurina* cell STS5 branched in among the *L. corrugata* sequences, and thus no phylogenetic separation was observed between the two morphotypes. *Keelungia* formed a maximally supported clade consisting of *Keelungia pulex* (Chan et al. 2013) and our sequence of *Keelungia* sp. strain KM082. The *Decastava* clade consisted of only one sequence, from *Decastava edaphica* (Cavalier-Smith et al. 2016). The '*Ploeotia* + *Serpenomonas*' clade (which we equate with the taxon Ploeotiidae) consisted of individual subclades of sequences belonging to *P. vitrea, P. oblonga,* and *S. costata*. As expected, our five new *Serpenomonas costata* and the three previously available sequences formed a maximally supported clade in all analyses (e.g. Figs 7, 8, and Supplementary Material Fig. A1). Within this clade, two maximally supported sub-clades were recovered, separating isolates with group I introns in their SSU-

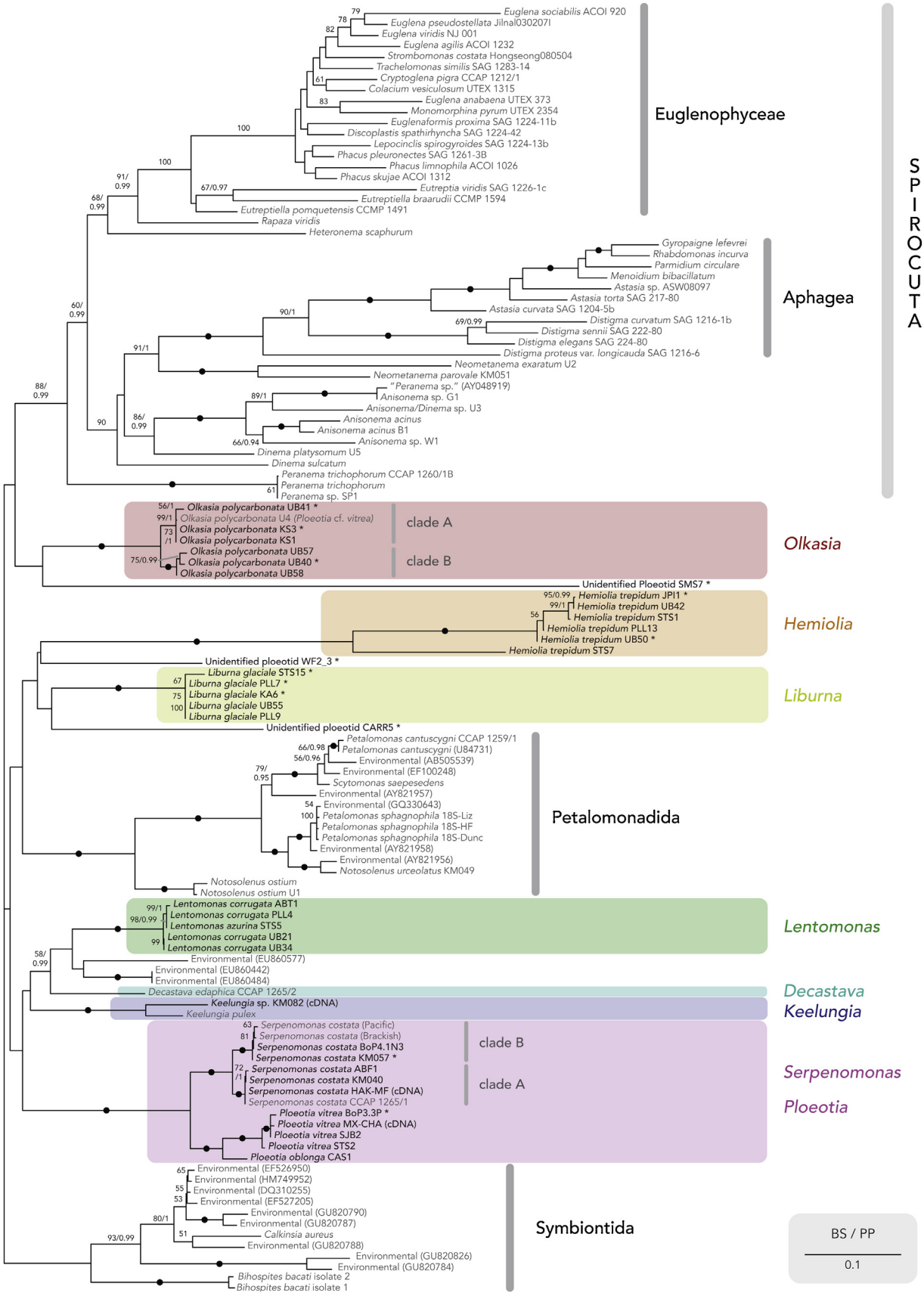
Euglena sociabilis ACOI 920
Euglena pseudostellata Jilnal030207I
Euglena viridis NJ 001
Euglena agilis ACOI 1232
Strombomonas costata Hongseong080504
Trachelomonas similis SAG 1283-14
Cryptoglena pigra CCAP 1212/1
Colacium vesiculosum UTEX 1315
Euglena anabaena UTEX 373
Monomorphina pyrum UTEX 2354
Euglenaformis proxima SAG 1224-11b
Discoplastis spathirhyncha SAG 1224-42
Lepocinclis spirogyroides SAG 1224-13b
Phacus pleuronectes SAG 1261-3B
Phacus limnophila ACOI 1026
Phacus skujae ACOI 1312
Eutreptia viridis SAG 1226-1c
Eutreptiella braarudii CCMP 1594
Eutreptiella pomquetensis CCMP 1491
Rapaza viridis
Heteronema scaphurum
Euglenophyceae
Gyropaigne lefevrei
Rhabdomonas incurva
Parmidium circulare
Menoidium bibacillatum
Astasia sp. ASW08097
Astasia torta SAG 217-80
Astasia curvata SAG 1204-5b
Distigma curvatum SAG 1216-1b
Distigma sennii SAG 222-80
Distigma elegans SAG 224-80
Distigma proteus var. longicauda SAG 1216-6
Aphagea
Neometanema exaratum U2
Neometanema parovale KM051
"Peranema sp." (AY048919)
Anisonema sp. G1
Anisonema/Dinema sp. U3
Anisonema acinus
Anisonema acinus B1
Anisonema sp. W1
Dinema platysomum U5
Dinema sulcatum
Peranema trichophorum CCAP 1260/1B
Peranema trichophorum
Peranema sp. SP1
SPIROCUTA
Olkasia polycarbonata UB41 *
Olkasia polycarbonata U4 (Ploeotia cf. vitrea)
Olkasia polycarbonata KS3 *
Olkasia polycarbonata KS1
clade A
Olkasia polycarbonata UB57
Olkasia polycarbonata UB40 *
Olkasia polycarbonata UB58
clade B
Olkasia
Unidentified Ploeotid SMS7 *
Hemiolia trepidum JPI1 *
Hemiolia trepidum UB42
Hemiolia trepidum STS1
Hemiolia trepidum PLL13
Hemiolia trepidum UB50 *
Hemiolia trepidum STS7
Hemiolia
Unidentified ploeotid WF2_3 *
Liburna glaciale STS15 *
Liburna glaciale PLL7 *
Liburna glaciale KA6 *
Liburna glaciale UB55
Liburna glaciale PLL9
Liburna
Unidentified ploeotid CARR5 *
Petalomonas cantuscygni CCAP 1259/1
Petalomonas cantuscygni (U84731)
Environmental (AB505539)
Environmental (EF100248)
Scytomonas saepesedens
Environmental (AY821957)
Environmental (GQ330643)
Petalomonas sphagnophila 18S-Liz
Petalomonas sphagnophila 18S-HF
Petalomonas sphagnophila 18S-Dunc
Environmental (AY821958)
Environmental (AY821956)
Notosolenus urceolatus KM049
Notosolenus ostium
Notosolenus ostium U1
Petalomonadida
Lentomonas corrugata ABT1
Lentomonas corrugata PLL4
Lentomonas azurina STS5
Lentomonas corrugata UB21
Lentomonas corrugata UB34
Lentomonas
Environmental (EU860577)
Environmental (EU860442)
Environmental (EU860484)
Decastava edaphica CCAP 1265/2
Decastava
Keelungia sp. KM082 (cDNA)
Keelungia pulex
Keelungia
Serpenomonas costata (Pacific)
Serpenomonas costata (Brackish)
Serpenomonas costata BoP4.1N3
Serpenomonas costata KM057 *
clade B
Serpenomonas costata ABF1
Serpenomonas costata KM040
Serpenomonas costata HAK-MF (cDNA)
Serpenomonas costata CCAP 1265/1
clade A
Serpenomonas
Ploeotia vitrea BoP3.3P *
Ploeotia vitrea MX-CHA (cDNA)
Ploeotia vitrea SJB2
Ploeotia vitrea STS2
Ploeotia oblonga CAS1
Ploeotia
Environmental (EF526950)
Environmental (HM749952)
Environmental (DQ310255)
Environmental (EF527205)
Environmental (GU820790)
Environmental (GU820787)
Calkinsia aureus
Environmental (GU820788)
Environmental (GU820826)
Environmental (GU820784)
Bihospites bacati isolate 2
Bihospites bacati isolate 1
Symbiontida
BS / PP
0.1

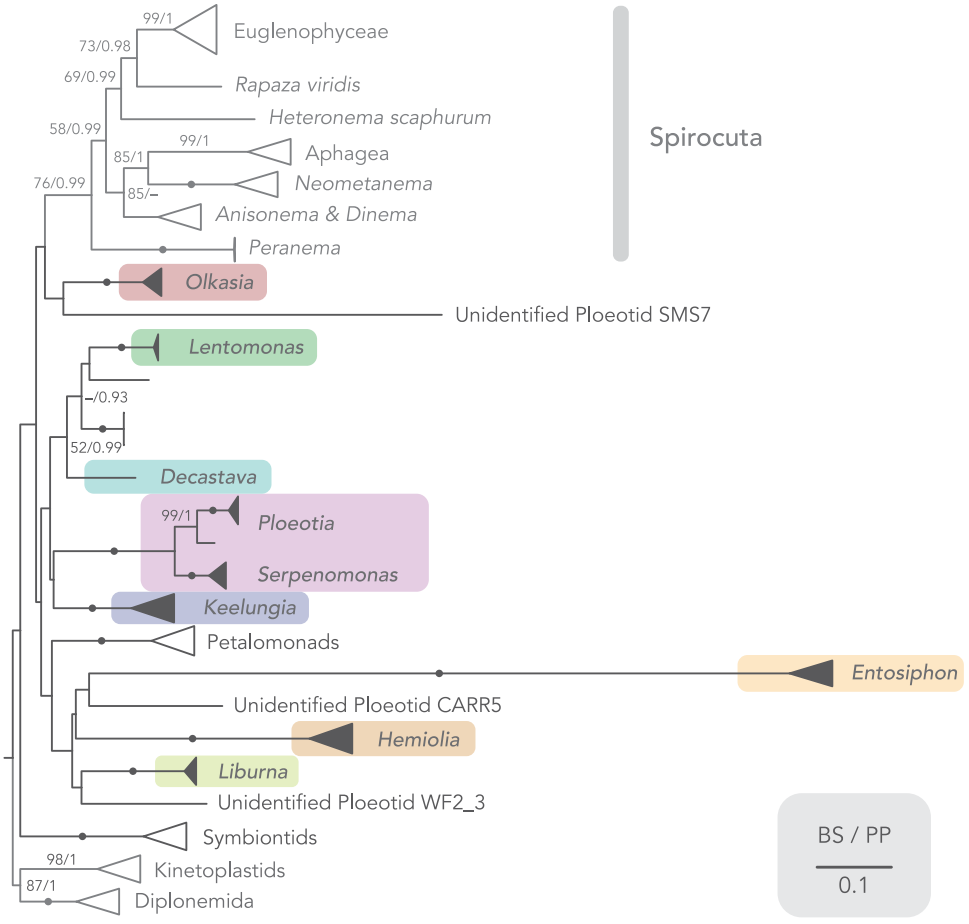

Figure 8. Summary view of euglenid phylogeny including *Entosiphon*, using the SSU-rRNA gene as inferred in maximum likelihood and Bayesian analyses (GTR + Γ model). Major groups of ploeotids are shown as collapsed, filled triangles. This tree is rooted on an outgroup of kinetoplastid and diplonemid taxa. Maximum bootstrap support (100%) and posterior probability (pp of 1) is shown with a black circle, while support values below 50% and 0.9 pp are not shown.

rDNA sequences (clade A, includes strain CCAP 1265/1), from a clade without any group I introns (clade B, includes strain KM057; Fig. 9a). Intriguingly, clade A is composed of strains isolated from both coasts of North America and Europe, whereas clade B isolates are Asian and Caribbean. Sister to *Serpenomonas*, we recovered *Ploeotia vitrea* (four new sequences) and *Ploeotia oblonga* (one new sequence), the latter branching sister to *P. vitrea* with strong to full support (e.g. Fig. 7 and Supplementary Material Fig. A1). Some *P. vitrea* sequences included group I introns (see below, and Fig. 9). *Entosiphon* consists of a tight cluster of similar sequences. This clade was extremely long branching and therefore only included in some of our analyses to limit long branch attraction artifacts, as in several recent studies (Cavalier-Smith et al. 2016; Lax and Simpson 2013; Paerschke et al. 2017). The new sequence of *Entosiphon* sp. strain ESC was sister to a clade containing *E. oblongum*

Figure 7. Maximum likelihood phylogeny of the SSU-rRNA gene of euglenids under the GTR + Γ model, with posterior probabilities derived from the same model. Major groups of ploeotids are shown, with sequences acquired in this study bolded, an asterisk (*) denotes a partial sequences. This phylogeny is unrooted and excludes *Entosiphon*; for rooted phylogenies with inferred outgroups included, plus *Entosiphon*, see Fig. 8 and Supplementary Material Figure A.1. Maximum bootstrap support (100%) and posterior probability (pp of 1) is shown with a black circle. Support values below 50% and 0.9 pp not shown.

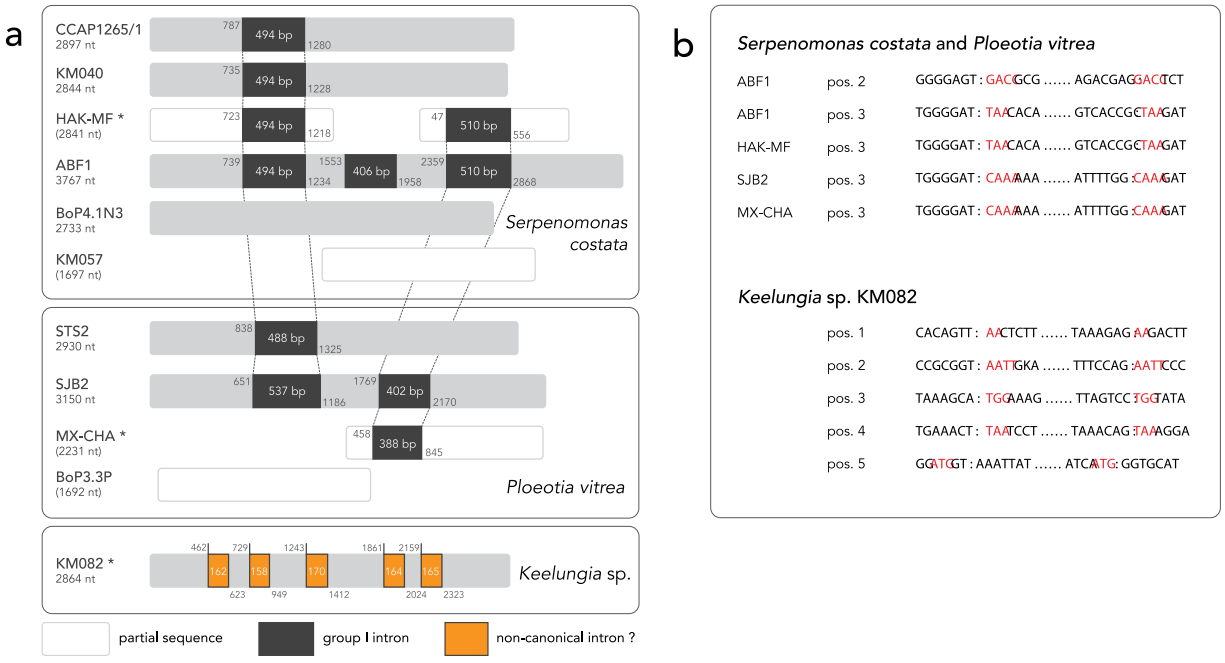

Figure 9. Introns in *Serpenomonas*, *Ploeotia* and *Keelungia* sp. (a) Positions of group I intron (dark grey) and possible non-canonical introns (orange) in the SSU-rRNA sequence of ploeotids. For taxa with white boxes, only partial SSU sequences were acquired. Lengths of introns are within boxes, with their start and end positions noted on either side. (b) Intron: exon boundaries of selected introns, at different positions (see a). Direct repeats are marked in red, and ":" shows the intron:exon boundary. Strains with * have had their SSU-rRNA sequence derived from cDNA as well as DNA. (For interpretation of the references to colour in this figure legend, the reader is referred to the web version of this article.)

and *Entosiphon* sp. strain TCS-2003, with moderate support (75% and 81%).

Relationship between clades

The exact relationships between the individual clades of ploeotids were poorly resolved and often differed between datasets and analyses (Supplementary Material Table A4). We recovered *Olkasia* branching as a sister to Spirocuta in all our datasets, although always with negligible support (Supplementary Material Table A4). Rogue taxon SMS7 branched with *Olkasia* in four of these analyses (Figs 7, 8). *Hemiolia* and *Liburna* formed a group to the exclusion of all other identified genera in five out of our six analyses, though with negligible support. In four cases, *Hemiolia* and *Liburna* (with or without *Entosiphon*—see below), form the sister group to Petalomonads, with little support (Supplementary Material Table A4). *Lentomonas* and *Decastava* formed a very poorly to moderately supported branch that also contained three partial-length environmental sequences when the latter were included (Fig. 7). The placement of *Keelungia* was unstable; in two analyses without *Entosiphon* it branched together with *Lentomonas* and *Decastava*, whereas in analyses including *Entosiphon* it grouped with *Ploeotia* and *Serpenomonas* (Fig. 8). In the analysis omitting short sequences, *Keelungia* branched with *Hemiolia*. None of these relationships was supported (Fig. 7). Ploeotiidae (*Ploeotia* + *Serpenomonas*), either alone or with *Keelungia*, formed a branch sister to the *Lentomonas* + *Decastava* + environmental sequences clade in five out of six analyses, with no support. In both analyses including *Entosiphon* support values were further reduced across the whole tree, likely owing to their long-branching nature (Fig. 8, Supplementary Material Table A4). *Entosiphon* formed a grouping including *Hemiolia* and *Liburna* in both, and this assemblage was in turn sister to petalomonads (see above).

Group I Introns

SSU-rRNA sequences derived from cDNA generated for *Serpenomonas costata* HAK-MF and *Ploeotia vitrea* MX-CHA were shorter than their DNA-derived counterparts. Alignment of RNA and DNA sequences showed a 494 bp intron in HAK-MF, at the same position as previously reported for *Serpenomonas costata* CCAP 1265/1 (Busse

and Preisfeld 2003). At the same position, isolates KM040 (*S. costata*, culture), ABF1 (*S. costata*, single cell), SJB2 (*P. vitrea*, culture), and STS2 (*P. vitrea*, single cell) also all showed similarly long introns. A 406 bp long intron was found only in ABF1 (*S. costata*, single cell) at a second position. A third intron site was found in HAK-MF (*S. costata*, culture), ABF1 (*S. costata*, single cell), MX-CHA (*P. vitrea*, culture), and SJB2 (*P. vitrea*, culture). Sizes ranged from 388 and 406 bp in *P. vitrea*, to 510 bp in *S. costata*. This last intron was confirmed with RT-PCR in both HAK-MF and MX-CHA. Introns at the second and third site had direct repeats at one end and in the opposite flanking region (Fig. 9b). The SSU-rDNA sequence of *Keelungia* sp. strain KM082 had five insertions that were missing from cDNA-derived SSU-rRNA sequences (Fig. 9a). These insertions were scattered along the whole length of the sequence, ranged from 158–170 bp, and were always found in conserved regions. All of these introns had 2–4 bp long direct repeats in one end of the intron and in the opposite flanking region, like in *Serpenomonas* and *Ploeotia* (Fig. 9b).

Original light microscopy images for all taxa, and, where available, scanning electron images are deposited in Dryad as https://doi.org/10.5061/dryad.k08pc1r, as are untrimmed alignments, trimmed alignments and treefiles for all phlylogenetic analyses. The new SSU-rDNA sequences reported here are deposited in GenBank as accessions MK239274–MK239309 and MK213404–MK213407.

Taxonomic Summary

This nomenclatural work has been registered in Zoobank, with the following LSID urn:lsid:zoobank.org:pub:5C4D3829-EA77-4E0B-AFF6-24D4-EBCC363D

Olkasia gen. nov. Lax, Lee, Eglit and Simpson (ICZN)

Description: Free-living, inflexible, biflagellate, heterotrophic euglenid, oblong in profile, ventrally flattened, with a conspicuous chisel-shaped feeding apparatus. The 10 pellicle strips are similarly sized, and S-shaped in cross-section (especially on the dorsal side), and overlap slightly with each other. Cells glide on their thickened posterior flagellum; and 'jerk back' when stressed. The anterior flagellum sweeps from side to side.

Type species: *Olkasia polycarbonata* Lax, Lee, Eglit and Simpson (description see below)

Etymology: From 'olkas' (Greek), a large trading barge used in Hellenistic times. Refers to the large size of the type species relative to *Ploeotia* (*Ploeotia* is from 'ploion' = boat in Greek). Feminine.

ZooBank Accession: LSID urn:lsid:zoobank.org:act:DBCD8D51-3766-4521-A1CD-4D91A-79CD317

Olkasia polycarbonata sp. nov. Lax, Lee, Eglit and Simpson (ICZN)

Description: Oblong cells, 54–63 by 30–37 μm, ventrally flattened.

Type material: The name-bearing type (hapantotype) is an SEM-stub with five osmium-fixed and sputter-coated single cells isolated by hand from the type locality. Deposited with the American Museum of Natural History, New York, as AMNH_IZC 00343283.

Type locality: Horseshoe Island Park, Halifax, Nova Scotia, Canada (N44°38′23.4″, W63°36′45.2″), oxic intertidal sediment.

Etymology: After 'polycarbonate', the transparent thermoplastic polymer [originally 'poly' = many (Greek), 'carbo' = coal, charcoal (Latin)]. Polycarbonate is often used instead of glass for windows, windscreens, etc. Refers to previous appellation of the organism as *Ploeotia* cf. *vitrea* (i.e. similar to *P. vitrea*), from 'vitrum' = glass (Latin).

Gene sequence: The partial SSU-rDNA sequence of a single cell (UB41) collected from the same sample as the hapantotype, at the same time, has the Genbank accession number MK239294.

ZooBank Accession: LSID urn:lsid:zoobank.org:act:22D0646E-BEA5-4556-AEF9-824A5C7F83EB

Hemiolia gen. nov. Lax, Lee, Eglit and Simpson (ICZN)

Description: Free-living, inflexible, biflagellate euglenids, oblong in profile, moderately dorsoventrally flattened. Cells glide rapidly on their thickened, >3X cell length posterior flagellum and with the anterior flagellum held to the right side and trembling. Movement occasionally arrests for a couple of seconds, then continues in same direction. Feeding apparatus not observed with light microscopy. Pellicle strip margins difficult to observe by light microscopy. Phylogenetically more closely related to *Hemiolia trepidum* than to *Liburna glaciale*.

Type species: *Anisonema trepidum* Larsen 1987 (=*Hemiolia trepidum*, comb. nov.)

Etymology: 'Hemiolia' (Greek) was a type of fast, light attack and scouting ship with one and a half banks of oars per side, used by pirates and navies in the Hellenistic era (from 'hemiolis' – one and a half). Refers to the speed and small relative size of cells (see *Liburna*, below). Feminine.

ZooBank Accession: LSID urn:lsid:zoobank.org:act:0A97EDBC-808D-4DDB-BE94-DFC-83907D046

Transfer of existing species to *Hemiolia*

Hemiolia trepidum (Larsen 1987) Lax, Lee, Eglit and Simpson comb. nov.

Basionym: *Anisonema trepidum* Larsen, 1987 (594–595, Fig. 6)

Liburna gen. nov. Lax, Lee, Eglit and Simpson (ICZN)

Description: Free-living, inflexible, biflagellate euglenids, oblong in profile, moderately flattened dorso-ventrally. Cells glide rapidly on their thickened, hook-shaped posterior flagellum (3X cell length). The anterior flagellum is held to the right side and trembles. Feeding apparatus not observed with light microscopy. Pellicle strip margins difficult to observe by light microscopy; apparently >10 strips. Type species is larger than that of *Hemiolia*, with which it shares most characteristics. Phylogenetically more closely related to *Liburna glaciale* than to *Hemiolia trepidum*.

Type species: *Anisonema glaciale* Larsen and Patterson 1990 (=*Liburna glaciale*, comb. nov.)

Etymology: 'Liburna' (Latin) was a fast attack ship with two banks of oars widely used in the Roman navy from the late Republic onwards. Refers to the speed and size of cells (see *Hemiolia*, above). Feminine.

ZooBank Accession: LSID urn:lsid:zoobank.org:act:691C514A-78C8-4E39-9D4D-2F793CFA2D42

Transfer of existing species to *Liburna*

Liburna glaciale (Larsen and Patterson 1990) Lax, Lee, Eglit and Simpson comb. nov.

Basionym: *Anisonema glaciale* Larsen and Patterson, 1990

Discussion

Molecular Phylogenetics of Phagotrophic Euglenids

Ever since the first sequence data from a phagotrophic euglenid was acquired, taxon sampling has slowly increased, and gradually advanced our understanding of euglenid phylogenetics (Breglia et al. 2007; Busse et al. 2003; Cavalier-Smith et al. 2016; Lax and Simpson 2013; Montegut-Felkner and Triemer 1997). It has become increasingly clear that flexible taxa with >12 pellicle strips indeed form a major derived clade within euglenids, as had been inferred primarily from morphology (Leander et al. 2001a, b)—this taxon, Spirocuta (or Helicales), includes a variety of phagotrophic euglenids in addition to phototrophs and osmotrophs (Cavalier-Smith 2016; Lee and Simpson 2014a; Paerschke et al. 2017). Within Spirocuta, *Neometanema* was established as representing the sister group to osmotrophs (Lax and Simpson 2013; Lee and Simpson 2014a), whereas outside Spirocuta, petalomonads have consistently been recovered as a clade (e.g. Cavalier-Smith et al. 2016; Kim et al. 2010; Lee and Simpson 2014b). Also, symbiontids were defined as a significant monophyletic group, either within euglenids, or sister to them (Breglia et al. 2010; Cavalier-Smith 2016; Lax and Simpson 2013). Within this context, the molecular examination of ploeotids stands out as having raised more questions than it answers. Incremental improvements in taxon sampling supported the notion that ploeotids likely represented several distinct clades with difficult-to-resolve relationships (Cavalier-Smith et al. 2016; Chan et al. 2013, 2015; Lax and Simpson 2013), but it remained essentially unknowable how many major clades there are. With this, any inferences about the deep-level phylogeny and evolution of euglenids were inevitably based on unreliably supported relationships and conjectural extrapolation to incorporate taxa with no molecular data (e.g. Cavalier-Smith 2016). It is this profound uncertainty that we aimed to reduce by increasing the taxonomic breadth of sequence data available for ploeotids.

Ploeotia, Serpenomonas and *Olkasia*

We resolved a central problem in the molecular biodiversity of ploeotids, by sequencing SSU-rDNA from *Ploeotia vitrea*, type species of *Ploeotia*. The phylogenetic position of *P. vitrea* was surprising given recent studies, being remote from '*Ploeotia* cf. *vitrea*' (Lax and Simpson 2013) but close to *Serpenomonas*, which was recently inferred to differ markedly from *Ploeotia* on morphological grounds (Cavalier-Smith et al. 2016; Cavalier-Smith 2016). The major consequences for the systematics of euglenids are discussed below.

The previously undescribed morphospecies identified as *Ploeotia* cf. *vitrea* by Lax and Simpson (2013) was considered to be similar to *Ploeotia vitrea*, but much larger, based on light microscopy observations. However, our molecular phylogenetic analyses including *P. vitrea* clearly show that it is not closely related to this *Ploeotia* cf. *vitrea*. In addition, our investigation with SEM revealed that the organization and linking between strips is distinctly different in the two taxa (compare

Fig. 2a, c with Fig. 5a, b). Based on the strongly supported phylogenetic placement outside the *Ploeotia-Serpenomonas* clade, as well as the morphological differences, we propose a novel genus and species, *Olkasia polycarbonata*, for *Ploeotia* cf. *vitrea* sensu Lax and Simpson (2013).

Surprisingly, our phylogenetic analyses strongly placed *P. oblonga* as sister to *P. vitrea* (Fig. 7). *Ploeotia oblonga* was previously considered to be closely allied to *Serpenomonas costata* based on light microscopy, in particular the alternating wide and narrow pellicle strips (e.g. Al-Qassab et al. 2002; Fig. 4k in Patterson and Simpson 1996). Our SEM investigation confirmed that the arrangement of alternating pellicle strips is similar to *S. costata*, but showed that the strip connections were located on raised keels, similar to *P. vitrea* (whereas these boundaries are folded over in *S. costata*; Farmer and Triemer 1988).

Serpenomonas costata/Ploeotia costata is closely related to *Ploeotia vitrea* and *P. oblonga*, such that it is a subjective decision whether to assign this taxon to the genus *Ploeotia* (Farmer and Triemer 1988; Larsen and Patterson 1990) or to a separate genus, *Serpenomonas* (Cavalier-Smith 2016; Triemer 1986). We recommend *Serpenomonas*, since we anticipate that future researchers will favour a larger number of narrower genera: Currently broadly 'defined' morphospecies will likely be subdivided into separate species taxa based on their divergent molecular sequences (e.g. *S. costata* or *O. polycarbonata*, Fig. 7). It is also likely that many more morphospecies of ploeotids will be found with more comprehensive taxon sampling. These increases in species will likely push genera to be less encompassing.

Some *Anisonema* Species are 'Ploeotids'

Our analyses, and several previous investigations, place *Anisonema* within Spirocuta with strong support (e.g. Lax and Simpson 2013; Paerschke et al. 2017). This is based on sequences from several different *Anisonema* isolates (Busse et al. 2003; Lax and Simpson 2013), most of them very similar to (or the same as) *Anisonema acinus*, which represents the type for the genus. Nonetheless, *Anisonema* has had a broad morphological identity—cells with widely spaced and almost longitudinal pellicle strips, gliding on the posterior flagellum, with the feeding apparatus not seen by light microscopy (Larsen 1987; Larsen and Patterson 1990; Lee and Patterson 2000)—and it has been unclear whether it represents a natural group (Larsen 1987; Lee and Patterson 2000). In our analyses, cells of *Hemiolia trepidum* (formerly *A. trepidum*) and *Liburna glaciale* (formerly *A. glaciale*) robustly fall outside Spirocuta (Figs 7, 8). *Anisonema* species differ in their flexibility, and while *A. acinus* is often reported to be slightly flexible when compressed or stressed (Lee et al. 2005), both *Hemiolia* and *Liburna* are more rigid (Larsen 1987), consistent with their phylogenetic placement.

Hemiolia and *Liburna* share several unusual characteristics: Unlike *A. acinus*, both are fast gliders with their anterior flagellum held to the right side, trembling rapidly (hence 'trepidum' = trembling), and often freezing for a few seconds before resuming movement (hence 'glaciale' = ice; Larsen 1987; Larsen and Patterson 1990). *Hemiolia* and *Liburna* mostly jerk back when stressed and always change direction when doing so, hold their cell bodies close to the surface, and exhibit smooth gliding (see Supplementary Material Videos 5 and 6), while *A. acinus* (for example) often moves erratically, frequently jerking backwards (e.g. Larsen 1987).

Within the ploeotid context, the particular locomotion behaviour of *Hemiolia* and *Liburna* is again distinctive, as is their feeding apparatuses not being visible by light microscopy (Larsen and Patterson 1990; Lee and Patterson 2000). With these similarities, it is perhaps surprising that *Hemiolia* and *Liburna* show considerable SSU-rDNA sequence divergence between them, and while *Hemiolia* and *Liburna* branch together in all our analyses, this relationship is never supported statistically (Figs 7, 8). For this reason, and bearing in mind recent splitting approaches to ploeotid taxonomy (Cavalier-Smith 2016), we propose to make *Anisonema trepidum* the type of a novel genus, *Hemiolia*, and *Anisonema glaciale* the type of a second new genus, *Liburna*. It is possible that *Hemiolia* and *Liburna* may have differing pellicle arrangements: It has been estimated previously that there are 6–7 strips in *Hemiolia trepidum*, and 12–15 in *Liburna glaciale* (Ekebom et al. 1995; Lee and Patterson 2000). A large number of strips in *Liburna* is consistent with our observations of 5–6 strip joints on the dorsal side of *L. glaciale*. Nonetheless, the strips are difficult to observe in both taxa, and accurate counts will likely require electron microscopy data. At present *Hemiolia* and *Liburna* (or at least their type species) are most reliably distinguished by size (Supplementary Material Table A2; Larsen and Patterson 1990; Lee and Patterson 2000).

The phylogenetic placement of *Liburna* and *Hemiolia* demonstrates that the morphological boundaries in the genus *Anisonema* are dubious, as long suspected (Larsen and Patterson 1990). In the future it is possible that other morphotypes

currently in *Anisonema* will also need to be moved to other genera. Additional molecular phylogenetic studies are needed to increase taxon sampling in this group, and to properly place its current members in a phylogenetic context.

Higher-order Systematics

Most work on ploeotids has examined their diversity and/or phylogeny, and until recently there were essentially no treatments of their higher systematics. However, Cavalier-Smith (Cavalier-Smith 2016; Cavalier-Smith in Cavalier-Smith et al. 2016) proposed a system of 18 higher taxa from the level of family up to infraphylum, that grouped together genera of ploeotids, or some ploeotids with other subgroups of euglenids. This was based on the sequence data available at the time, plus some inferences from morphology. Several unusual aspects of this system are important for context: 15 of the taxa were new, all the 'families' contained a single genus, one new taxon was explicitly envisaged as a paraphyletic group, and none of the other taxa for which there were data from >1 ploeotid genus corresponded to a strongly supported clade in Cavalier-Smith's (2016) own SSU-rDNA phylogenies. Startlingly, none of the proposed higher taxa containing >1 ploeotid genus form even a weakly supported clade in our analyses with their current compositions.

The monophyly of some of the proposed major taxa is strongly disconfirmed by our phylogenies. In particular, the class Ploeotarea and order Ploeotiida group *Ploeotia* with *Lentomonas* only, while class Stavomonadea groups *Serpenomonas* with petalomonads, *Keelungia* and *Decastava* (Cavalier-Smith 2016). This dichotomy sharply conflicts with the strongly supported close relationship between *Ploeotia* and *Serpenomonas* to the exclusion of *Lentomonas*, petalomonads, *Keelungia* and *Decastava*. This situation stems mainly from Cavalier-Smith (2016) assuming that *Ploeotia vitrea* is closely related to *Ploeotia* cf. *vitrea* sensu Lax and Simpson (2013; now *Olkasia polycarbonata*), which proves not to be the case. The assignment of *Lentomonas* to Ploeotarea and Ploeotiida was made without molecular data, apparently on the basis of similar pellicle and feeding apparatus structure (see Diagnosis of Ploeotarea in Cavalier-Smith 2016). Given the closer relationship of *Ploeotia* with *Serpenomonas*, these similarities at best identify a broader group than *Ploeotia* plus *Lentomonas*. The close relationship between *Serpenomonas* and *Ploeotia* also argues against assigning *Serpenomonas* to its own subclass Heterostavia, order Heterostavida and family *Serpenomonadidae*, especially since the heterostavous condition is also seen in *Ploeotia oblonga* (see below).

Meanwhile, another set of taxa in Cavalier-Smith's (2016) system were not strongly contradicted by our analyses, but nonetheless were never recovered as clades, irrespective of whether the three new genera we propose are considered. These unsupported taxa include the subclass Homostavia (uniting *Decastava* and *Keelungia* with petalomonads), order Decastavida (uniting *Decastava* and *Keelungia*), and superclass Rigimonada (uniting all ploeotids and petalomonads, to the exclusion of *Entosiphon*), though the latter was actually envisaged as paraphyletic (Cavalier-Smith 2016). We also did not recover *Entosiphon* as a sister clade to all other euglenids (excluding symbiontids, Fig. 8) as implied by the division of euglenids into two infraphyla: Entosiphona (*Entosiphon* only), and Dipilida (all other euglenids). *Entosiphon* represents an extremely long branch in SSU-rDNA phylogenies, and this marker is widely recognised as unreliable for inferring the placement of this genus (Busse et al. 2003; Cavalier-Smith et al. 2016; Paerschke et al. 2017; von der Heyden et al. 2004). Unfortunately, our study confirms that SSU-rDNA is currently the only marker with taxon sampling anywhere near rich enough to credibly address the deepest phylogenetic divisions within euglenids. Thus, while the Entosiphona/Dipilida distinction draws mainly on Hsp90 phylogenies and morphological arguments, rather than SSU-rDNA analyses (Cavalier-Smith 2016; Cavalier-Smith et al. 2016), the only ploeotids in those Hsp90 phylogenies are *Entosiphon* and *Decastava*.

As a result of our investigations, the entire systematisation above the level of family involving ploeotid taxa proposed by Cavalier-Smith (2016) seems to be without utility. The system was proposed on the basis of weak phylogenetic evidence in the first place, and—with the benefit of additional data—proves to be largely (likely entirely) incompatible with the widely held ideal of higher taxa being monophyletic where possible. Even with the improved taxon sampling of our study, the deep-level phylogenetic relationships amongst euglenids remain unresolved, and any replacement proposal for supra-familial taxa (or dramatic alteration of the concepts applying to existing names) runs an unacceptably high risk of a similar incompatibility. Systematics should wait until repeatable, strongly supported molecular phylogenetic results are obtained; for euglenids these are likely to be

available soon, through low-cost transcriptomics (see below).

Serpenomonas and *Ploeotia* turn out to be very closely related and genetically similar, such that it is a more-or-less subjective decision whether to regard them as separate genera (see above). We anticipate that assigning them to the same family will be non-controversial. We propose Ploeotiidae Cavalier-Smith 2016, rather than Serpenomonadidae Cavalier-Smith 2016, since *Ploeotia* Dujardin 1841 has priority over *Serpenomonas* Triemer 1986. This would minimise confusion if *Ploeotia* and *Serpenomonas* were considered synonymous in the future.

The presence or absence of an unpaired U nucleotide in conserved helix 44 of the V9 region of SSU rRNA has recently been identified as a character that is potentially relevant to euglenid phylogenetics (and systematics), and specifically provides some evidence for a Spirocuta + *Entosiphon* grouping (Paerschke et al. 2017). This unpaired U is present in more basal euglenids like petalomonads, *Serpenomonas costata*, *Keelungia*, and *Olkasia*, but not in Spirocuta or *Entosiphon* (Paerschke et al. 2017). As expected, all new sequences of *S. costata*, *Ploeotia vitrea* and *P. oblonga*, *Keelungia*, and *O. polycarbonata* have the unpaired U (data not shown). This nucleotide is absent from *Entosiphon* sp. ESC (as expected), but also not present in *Lentomonas*, *Hemiolia* and unidentified ploeotid WF2_3. Meanwhile, *Liburna* sequences have two unpaired Us at this position. We conclude that the absence of this unpaired base is more widespread in euglenids than was previously supposed. While this character might still represent a synapomorphy of a group including Spirocuta + *Entosiphon*, it is more likely that it has a complex evolutionary history. The unresolved branching order of euglenids currently inhibits any further analysis past speculation.

Phylogenetic Structure within Morphospecies

At present, most heterotrophic euglenid species are defined by morphology applied at the light microscopy level, with the majority of broad morphospecies distinctions based on criteria like cell shape and size, surface structure, flexibility and whether the feeding apparatus is visible (e.g. Lee 2012). We now have sufficient molecular sampling for a few ploeotid morphospecies to investigate their sequence divergence and phylogenetic structure more closely. *Serpenomonas costata* is split into two maximally supported, distinct subgroups (Fig. 7): clade A (taxa from North America/Europe, includes the type strain CCAP 1265/1), and clade B (taxa from Asia/Caribbean, includes strain KM057). Intriguingly, taxa in clade A all have group I introns, whereas none were found in clade B (see below; Fig. 9). This finding is largely consistent with Chan et al. (2015), who reported *S. costata* sequences isolated from Taiwan. This tentative biogeographical separation could be an artefact of still-modest taxon sampling, but is worth further investigation. Sequence identity within both clades was high, but was only 73.3–75.8% between clade A and B isolates (considering full-length sequences without introns). *Olkasia* is also split into moderately supported A and B clades (Fig. 7). The two *Olkasia* clades are certainly not biogeographically distinguished since both have been found at one site in Nova Scotia, Canada. Sequence identities within clades A and B were high (97.9 and 99.1%), while identity was 90.6–93.5% between clades (Supplementary Material Table A3). It is probable that *Serpenomonas costata* will be split up into at least two nomenclatural species in the future, and possible that *Olkasia polycarbonata* will be as well.

Conversely, *Lentomonas corrugata* and *L. azurina* sequences do not form separate clades in SSU-rRNA gene phylogenies. There is no clear distinction in their SSU-rRNA gene identities: 97.2–99.8% of sites between *L. corrugata* and *L. azurina* are identical, while there is 95–99.8% identity amongst different *L. corrugata* cells. *Lentomonas azurina* was originally distinguished from *L. corrugata* by being substantially more slender (Patterson and Simpson 1996), and a sharp distinction in length:width ratio was observed in the cells we examined (Supplementary Material Table A2). It is possible that the *L. corrugata* morphospecies gave rise to the *L. azurina* morphospecies, or they could also represent a single species, with *L. azurina* representing a rarer life cycle stage of *L. corrugata*. It is also unclear how much morphological variation is seen within clones of *Lentomonas* morphotypes, especially in length:width ratio. It is also possible that our STS5 cell was an aberrant or unhealthy cell, not representative of 'true' *L. azurina*. More comprehensive molecular sampling of this group, especially the less commonly observed *L. azurina*, is needed to resolve these issues, ideally from different geographic locations, and with the use of cultures.

Pellicle Strip Architecture

Broadly speaking, differences in the organisation of individual pellicle strips seem to distinguish the

major phylogenetic groupings of ploeotids, which is consistent with patterns seen in other euglenids, especially phototrophs (Leander et al. 2007; Yubuki and Leander 2012). For example, taxa with straight, bifurcating keels (strip boundaries on raised keels) fall within *Ploeotia*. The closely related taxon *Serpenomonas* also has bifurcations, though they are at the edges of a trough-like structure made by the narrow strips. In contrast, *Lentomonas* has raised bifurcating ridges (dorsal side only) with strip joints located on one side of the ridges (i.e. not straight, like in *Ploeotia*). Nonetheless, pellicle strips need to be examined carefully, and while light microscopy is easily accessible, scanning electron microscopy helps greatly in understanding the organization of strips (Esson and Leander 2006). One example is *P. oblonga*: it has previously been thought that this morphospecies is most closely allied with *S. costata* (Larsen and Patterson 1990; Lee and Patterson 2000; Lee 2008), since *P. oblonga* resembles *S. costata* in having alternating thin and wide strips. Our SEM analyses revealed that the strip boundaries are considerably different in *P. oblonga*, being raised on keels like in *P. vitrea* (Fig. 2).

It is likely that pellicle strip structure has a complex evolutionary history within ploeotids, for example the alternation of narrower and wider strips likely arose at least three times independently: in *Ploeotia oblonga, Serpenomonas,* and, arguably, *Entosiphon* (it is also possible it arose twice, and was subsequently lost in *Ploeotia vitrea*). This alternation in strip width could be explained by pellicle strip morphogenesis during cell division. Cavalier-Smith (2017) reinterpreted data from Triemer and Fritz (1988), Leander and Farmer (2001) and Leander et al. (2007). He inferred that during division of *S. costata*, the narrow strips mature into wide strips, and ten new narrow strips inserted at their flanks (Cavalier-Smith 2017). If so, this process may help explain the occurrence of heteromorphic pellicle strips in multiple taxa of ploeotids including *P. oblonga*, since it is—in principle—a simple difference in pellicle strip development timing (heterochrony). This phenomenon has been inferred to explain pellicle whorl patterns in phototrophic euglenids (Esson and Leander 2006; Leander et al. 2007; Esson and Leander 2008). Further cell-developmental investigations of *Serpenomonas*, *Entosiphon* and/or *P. oblonga* (and other taxa with heteromorphic strips) would be illuminating.

Our SEM observations show that *Olkasia* has S-shaped pellicular strips, with the joints between strips lying under an overhang. Of all ploeotid groups examined so far, this is arguably the most similar to the strip morphology of typical spirocutes (Leander et al. 2001a). In addition, the chisel-shaped feeding apparatus of *Olkasia* differs from the hook-shaped apparatus seen in the other ploeotids sequenced to date in which the feeding apparatus is clearly visible, other than the special case of *Entosiphon* (Cavalier-Smith et al. 2016; Chan et al. 2013; Lee 2008). Chisel-shaped feeding apparatuses are common in phagotrophic spirocutes, as well as in some ploeotids for which there are no sequence data (Larsen and Patterson 1990; Lee 2008). These similarities are worth further examination, especially bearing in mind that *Olkasia* branches as a sister group to spirocutes in our phylogenetic analyses (with negligible support), as well as in some other recent analyes (Cavalier-Smith 2016), although not in all (Paerschke et al. 2017).

Eukaryotrophy in Ploeotids

It has been proposed that phagotrophic euglenids were ancestrally bacterivorous and that the development of a flexible pellicle in an ancestor of Spirocuta was needed for phagotrophic euglenids to become effective eukaryotrophs (Leander et al. 2001a; Leander 2004). This eukaryotrophy subsequently enabled a phagotrophic euglenid to participate in secondary endosymbiosis as the host (Leander et al. 2001a). This association has been questioned, however (Cavalier-Smith 2016; Lax and Simpson 2013), and our study provides further evidence that some rigid euglenid taxa (like ploeotids) can be effective eukaryotrophs. All of the *Olkasia* cells we isolated contained ingested algae (Fig. 4), as did the cell studied by Lax and Simpson (2013). Further, we observed ingested algal material in *Ploeotia vitrea, P. oblonga, Entosiphon* sp. (Figs 1f–h and 6m, n), *Keelungia* sp., and *Serpenomonas costata*, with the latter already reported to be able to ingest algae and other eukaryotic cells (Linton and Triemer 1999). In this study we also demonstrated that some taxa formerly assigned to *Anisonema* branch outside Spirocuta. These taxa, *Hemiolia* and *Liburna*, seem to include accomplished eukaryotrophs: Several of our isolated cells of *Hemiolia* and *Liburna* contained whole ingested pennate diatoms up to 19 μm in length (Fig. 6e, i–k). Both *Hemiolia* and *Liburna* have previously been reported to contain ‘small granules’ (Lee and Patterson 2000; Lee 2008), which might be ingested prey, as mentioned as a possibility in the original description (Larsen 1987). We conclude that the ability to ingest smaller eukaryotes is widespread among ploeotids sensu lato.

Group I and Non-canonical Introns

A group I intron was discovered in *Serpenomonas costata* strain CCAP 1265/1 by Busse and Preisfeld (2003). Chan et al. (2015) subsequently sequenced two additional *Serpenomonas* isolates that lacked group I introns. With further sampling we found group I introns across *Serpenomonas* clade A, which includes CCAP 1265/1, but did not find any in clade B, to which Chan et al's sequences belong (Fig. 9a; see above). Interestingly, we also found a group I intron of similar length at the same position in some of our *Ploeotia vitrea* isolates (Fig. 9a).

Gain and loss of a group I intron is known as the Goddard-Burt cycle (Goddard and Burt 1999; Haugen et al. 2005), and is initiated with a cutting site created by a homing endonuclease (HE). This evolutionary process means that soon after gain of the intron, the HE-gene is still present, but is subsequently truncated prior to loss. Homing endonuclease genes were absent from the introns in *S. costata* clade A and *P. vitrea*, suggesting that these are in the loss phase of the cycle. A phylogenetic analysis based on the dataset of Busse and Preisfeld (2003) showed that the *P. vitrea* group I intron is not specifically related to that in *S. costata* (data not shown). It is thus likely that these introns invaded *Serpenomonas* and *Ploeotia* independently (and *S. costata* clade B may never have been invaded), which is consistent with the genetic divergence between *Ploeotia* and *Serpenomonas*.

We were not able to detect any additional group I or II intron sequences at other positions with RNAweasel (see Methods), but the SSU-rDNA alignment showed conspicuous insertions at two other positions in some *Serpenomonas costata* and *Ploeotia vitrea* isolates, and we confirmed in two cases that these insertions are absent from the rRNA (Fig. 9a). We inferred the secondary structures of these introns and found at least 8 of the 10 conserved core domains (P2–P9; data not shown) that are characteristic of group I introns (Haugen et al. 2005). In the phylogenetic analysis with group I introns mentioned above, sequences from these positions formed a clade that was clearly separate from the introns at position 1.

In addition, we recorded five 158–170 bp long inserts in *Keelungia* sp. strain KM082, which did not share positions with the introns in *S. costata* and *P. vitrea* (Fig. 9a). These insertions were not present in cDNA-derived SSU-rRNA sequences, suggesting that they are also introns. While group I introns shorter than 200 bp have been found (Zhou et al. 2007), our RNAweasel analysis again did not identify them as group I or II introns or other related self-splicing entities, and we were not able to construct secondary structures. Additional examination showed that the introns at these positions have similarities to the non-canonical introns found in several protein-coding genes of euglenozoans, mainly *Euglena gracilis* (Breckenridge et al. 1999; Gumińska et al. 2018; Henze et al. 1995; Milanowski et al. 2014) and diplonemids (Gawryluk et al. 2016). Data for phagotrophic euglenids are sparse, but there are several short, non-canonical introns in the Hsp90 gene of the spirocute *Peranema trichophorum* (Breglia et al. 2007). In addition to possessing a stable secondary structure bringing both splicing sites together, these introns have short 2–4 bp direct repeats in one end of the intron and in the opposing end of the flanking region (Henze et al. 1995). We speculate that these features in KM082 *Keelungia* sp. might represent non-canonical introns. Non-canonical introns are common in protein-coding genes of euglenids (Breglia et al. 2007; Gumińska et al. 2018; Henze et al. 1995), but have not—to our knowledge—been reported in rRNA genes. More research into the distribution, structure, and splicing of these putative non-canonical introns is merited.

Have we Found All Major Clades of Ploeotids?

We here report sequences from ten different morphospecies of ploeotids, many of which were formerly assigned to genus *Ploeotia*, whereas there at least 22 described morphospecies in *Ploeotia* alone (for example see Al-Qassab et al. 2002; Larsen and Patterson 1990; Patterson and Simpson 1996). It is possible that some of these other species represent additional major clades of ploeotids, beyond the eight identified thus far. This is especially true for taxa with arrangements of pellicle strips that differ from those of the identified major clades and/or where the fine structure of strip joints is unknown, like *Ploeotia adhaerens* or *P. scrobiculata* (Larsen and Patterson 1990). Until molecular data are obtained from these morphospecies, their phylogenetic placement will remain highly uncertain: Their assignation to *Ploeotia* must be seen as provisional, but should be retained until clear evidence of their actual phylogenetic affinities is available.

The Need for Multigene Phylogenies

In all of our analyses ploeotids appear as paraphyletic, forming the base of the euglenid tree, if the question of the position and identity of symbiontids

is overlooked (Figs 7, 8). On its own, this suggests that a ploeotid-like organism could indeed be the ancestor from which all other euglenids arose, however the branching order amongst the major ploeotid clades was very poorly resolved and supported in our study. Although we now have a clearer picture of the number and diversity of the major groups of ploeotids, it is obvious that SSU-rDNA sequences alone will not resolve relationships between those groups. Multigene phylogenetics are likely needed to resolve deep euglenid phylogeny. This approach has been used successfully in a range of protist groups, including phototrophic euglenids (e.g. Karnkowska et al. 2015). In addition to using culture-based approaches, methods like single-cell transcriptomics have the potential to rapidly increase taxon sampling for phylogenomic studies, especially for taxa that are difficult to culture (Kolisko et al. 2014; Lax et al. 2018). Our identification of major groups of ploeotids is an important step in establishing what taxon sampling is appropriate for future phylogenomic analyses.

Methods

Cultures: Establishment and nucleic acid extraction: Marine intertidal sediments were used to establish crude cultures, with sterile seawater supplemented with 1–3% LB (v/v) as the initial medium (sample sites yielding euglenid cultures are reported in Table A5). Cultures of *Serpenomonas costata, Ploeotia vitrea, P. oblonga* and *Keelungia* sp. were obtained by serial dilution of crude cultures, or isolation of single cells with a pipette. After establishment, cultures were maintained in tissue culture flasks in ~10 ml sterile seawater supplemented either with 0.1–1% LB media (v/v) or a sterile barley grain, with transfers every 2–3 weeks. Cells of *Entosiphon* sp. were isolated from freshwater sediment into tap water to form a crude culture. The culture was then supplemented with *Haematococcus* sp. as prey, and transferred every 2–24 months. Cultures were imaged under coverslips with a Zeiss Axiovert 200M and AxioCam M5.

DNA from all cultures was isolated with a Qiagen DNAeasy Blood and Tissue kit, using the tissue protocol, and quantified via spectroscopy with a NanoDrop (Thermo Scientific). We also isolated mRNA from three cultures either using a TRIzol-based extraction, following the manufacturers' instructions (*S. costata* HAK-MF and *P. vitrea* MX-CHA; Thermo Life Sciences), or RNA spin-columns (*Keelungia* sp. culture KM082; Macherey-Nagel NucleoSpin RNA XS). Reverse transcription to cDNA was carried out with a template-switching oligo, as described by Picelli et al. (2013).

Single cells: Photodocumentation and DNA amplification: Preparation of marine sediment samples largely followed Larsen and Patterson (1990). Briefly, sediment was collected from various sites across North America (Supplementary Material Table A5), placed into small trays, and spread out to 1–2 cm thickness. Kimwipe tissue was added on top, then 50 × 20 mm glass coverslips. A transparent lid was added to reduce evaporation. After 12–72 h under ambient within-laboratory day-night cycle, the coverslips were examined bottom facing up with seawater added, on an inverted microscope (either Zeiss Axiovert 200M under 1000×; or Leica DM IL LED under 400× or 630× total magnification). Individual cells were imaged (with a Zeiss AxioCam M5 or a Sony NEX6, respectively), and then isolated by mouthpipetting with a drawn-out glass pipette. Cells were washed 3–5 times in 2 μl drops of sterile seawater under the microscope before being expulsed into separate 0.2 ml PCR tubes containing 9.5 μl PCR-grade distilled water. Cells were lysed by up to 10 freeze-thaw cycles (−80 °C and RT) and DNA was amplified by multiple displacement amplification (MDA), using an Illustra GenomiPhi v3 kit (GE Healthcare), following the manufacturer's instructions, but with the 30 °C isothermal amplification time extended to 2 h. Success of the MDA reactions was assessed by running 1 μl of the product on a 0.5% agarose gel.

PCR amplification and sequencing: SSU-rDNA fragments were amplified from DNA from cultures and cells by PCR, using a variety of different euglenid/ploeotid-biased primers (Supplementary Material Table A1). Primers biased towards ploeotids (including *Hemiolia* and *Liburna*) were designed by modifying previously published euglenid-biased primers (Busse et al. 2003; Lax and Simpson 2013), or scanning alignments of existing SSU-rDNA sequences for suitable conserved sites. Amplifications were carried out with Invitrogen Recombinant Taq, 2 mM $MgCl_2$, and 0.2 mM dNTPs. Initial denaturing was done at 95 °C for 3 min; then 35 cycles of: denaturing at 95 °C for 30 sec, annealing at 50–64 °C (see Supplementary Material Table A1 for primer combinations) for 30 sec, elongation at 72 °C for 2 min; and a final elongation step at 72 °C for 10 min. Products were visualised with gel-electrophoresis on a 1% agarose gel, and either sent directly for Sanger sequencing (Génome Québec) or first gel-extracted with a Qiagen Gel-Extraction kit. Almost full-length SSU-rDNA sequences were obtained for most cells/cultures by amplifying at least two overlapping fragments. Raw reads were quality-checked by eye and automatically assembled de novo using Geneious R10 (Kearse et al. 2012), then queried against the NCBI GenBank nr database to identify any contaminant sequences. For one cultured strain, *P. vitrea* MX-CHA, only a partial SSU-rDNA sequence was obtained by PCR amplification, but a full-length SSU rRNA was extracted from transcriptome data from the same strain. The methods for this Illumina sequencing will be reported elsewhere (Lax et al. unpublished).

Alignment and phylogenetic analyses: The new sequences were added to a seed alignment including 34 phagotrophic euglenid sequences available on GenBank, a phylogenetically broad selection of primary osmotrophic and phototrophic euglenids, and symbiontids. Representative sequences from diplonemids and kinetoplastids were included as outgroups. To exclude potential long-branch attraction artifacts we also created datasets without *Entosiphon* and/or without outgroups (four datasets total). To exclude potential reduced resolution due to short sequences, we created a fifth dataset without sequences <1000 bp. In a sixth dataset, we excluded CARR5, SMS7, WF2_3, *Heteronema*/*Teloprocta scaphurum*, and 13 other sequences, since they were identified as rogue taxa by RogueNaRok (Aberer et al. 2013) under the RNR algorithm. The base dataset was aligned with MAFFT E-INS-I (Katoh and Standley 2013), checked manually with AliView (Larsson 2014), and masked by eye with SeaView (Gouy et al. 2010) to exclude ambiguous positions for all five taxon selections. This yielded a 1276 nt trimmed alignment for the datasets with all taxa included (156 taxa) and all taxa minus outgroup (123 taxa). A 1360 nt trimmed alignment was

generated for the datasets without *Entosiphon* (151 taxa); without *Entosiphon* and outgroups (118 taxa); and without *Entosiphon*, short sequences; and rogue taxa (100 taxa). The 'all-taxa' dataset was also automatically trimmed with trimAl to test whether any major results could stem from user bias in site masking (Capella-Gutiérrez et al. 2009; −st 0.001 −gt 0.89; 1354 sites). For each dataset, Maximum Likelihood phylogenies were inferred with RAxML under the GTR + Γ model (Stamatakis 2014), with robustness assessed with 1000 bootstraps for each analysis. We also carried out Bayesian analyses on the main dataset and on the dataset with *Entosiphon* and with outgroups. MrBayes (Ronquist et al. 2012) was used under the GTR + Γ model, running 4 chains (default heating parameters) for 5,000,000 generations each, with trees sampled every 1000 generations and the first 25% discarded as burn-in. Convergence was confirmed by assessing that PRSF values (Potential Scale Reduction Factor) approached 1.0. The 'all-taxa' ML-derived trimAl tree was very similar to the dataset masked by eye, with none of the differing bipartitions receiving more than 50% BS support in either analysis.

Potential group I introns were identified by looking for conspicuous insertions in the alignment and then examining those sequences with RNAweasel (http://megasun.bch.umontreal.ca/RNAweasel/Accessed Nov. 5 2018). Conspicuously, RNAweasel did not identify possible introns in isolate ABF1 (*Serpenomonas costata*) or culture SJB2 (*Ploeotia vitrea*); despite these having 406 and 510 bp, and 402 bp insertions, respectively. We subsequently generated cDNA-derived SSU sequences for HAK-MF (*S. costata*), MX-CHA (*P. vitrea*), and KM082 (*Keelungia* sp.; see above). Sequences from both DNA and cDNA were aligned and compared to confirm that the insertions were excised from the rRNA. To investigate the presence or absence of homing endonuclease (HE), we blasted the intron sequences using BLASTx against the GenBank nr database.

Pairwise sequence identities were calculated from whole (unmasked) sequence alignments, but with intron sequences excluded. Partial sequences were excluded from reporting, unless specifically noted (all scores can be found in Supplementary Material Table A3).

Scanning electron microscopy: 50–100 μl of cells from ~2 week old cultures of *Serpenomonas costata* strain HAK-MF, *Ploeotia oblonga* strain CAS1, and *Ploeotia vitrea* strains BoP4.1PV and MX-CHA were transferred onto poly-L-lysine-coated 12 mm round coverslips, and immediately fixed with a drop of 25% glutaraldehyde and OsO_4 vapor, for 1 h. After fixation, the coverslips were washed 3× in filtered seawater or dH_2O, and then subjected to a dehydration series of ethanol-water mixtures, as follows: 30%, 50%, 70%, 80%, 90%, 95%, 100% (3×). This was followed by critical-point drying with CO_2 on a Leica EM CPD300, then a ~15 nm Au-Pd coat was added with a Leica EM ACE200 sputter-coater. Samples were imaged on Hitachi S4700 or Zeiss LEO 1455VP scanning electron microscopes.

Single cells of *Olkasia polycarbonata* were isolated by pipette from fresh samples, and dropped onto poly-L-lysine-coated coverslips with ~50 μl of filtered seawater and a drop of 25% glutaraldehyde. Fixation, dehydration and imaging followed the procedure described above. In order to associate these cells with a molecular identity, some cells of *O. polycarbonata* designated for molecular work (see above) were isolated from the same samples at the same time (i.e. presumably from the same populations).

Acknowledgements

We thank the Tula Foundation for supporting field work on Calvert and Quadra Island, CARMABI for enabling field work in Curaçao, Noriko Okamoto and Patrick Keeling (University of British Columbia) for help with sampling and use of their microscope while in the field, and to Michelle Leger for providing the source samples for cultures MX-CHA and ESC. We thank Ping Li and Pat Scallion (both Dalhousie University) for assistance with SEM-imaging, Michael Gray (Dalhousie University) for feedback on introns in euglenids, and Claire Burnard for some sampling assistance. The research was supported by NSERC grant 298366-2014 to AGBS, and by CIfAR. WJL was supported by grants from the National Institute of Biological Resources, Korea (NIBR201801202) and the National Research Foundation of Korea (NRF-2018R1A2A3075567).

Appendix A. Supplementary Data

Supplementary data associated with this article can be found, in the online version, at https://doi.org/10.1016/j.protis.2019.03.001.

References

Aberer AJ, Krompass D, Stamatakis A (2013) Pruning rogue taxa improves phylogenetic accuracy: an efficient algorithm and webservice. Syst Biol **62**:162–166

Adl SM, Bass D, Lane CE, Lukeš J, Schoch CL, Smirnov A, Agatha S, Berney C, Brown MW, Burki F, Cárdenas P, Čepička I, Chistyakova L, del Campo J, Dunthorn M, Edvardsen B, Eglit Y, Guillou L, Hampl V, Heiss AA, Hoppenrath M, James TY, Karpov S, Kim E, Kolisko M, Kudryavtsev A, Lahr DJG, Lara E, Le Gall L, Lynn DH, Mann DG, Massana i Molera R, Mitchell EAD, Morrow C, Park JS, Pawlowski JW, Powell MJ, Richter DJ, Rueckert S, Shadwick L, Shimano S, Spiegel FW, Torruella i Cortes G, Youssef N, Zlatogursky V, Zhang Q (2019) Revisions to the classification, nomenclature, and diversity of eukaryotes. J Eukaryot Microbiol **66**:4–119

Al-Qassab S, Lee WJ, Murray S, Simpson AGB, Patterson DJ (2002) Flagellates from stromatolites and surrounding sediments in Shark Bay, Western Australia. Acta Protozool **41**:91–144

Boenigk J, Arndt H (2002) Bacterivory by heterotrophic flagellates: community structure and feeding strategies. Antonie van Leeuw J Microb **81**:465–480

Breckenridge DG, Watanabe Y-I, Greenwood SJ, Gray MW, Schnare MN (1999) U1 small nuclear RNA and spliceosomal introns in *Euglena gracilis*. Proc Natl Acad Sci USA **96**:852–856

Breglia SA, Slamovits CH, Leander BS (2007) Phylogeny of phagotrophic euglenids (Euglenozoa) as inferred from Hsp90 gene sequences. J Eukaryot Microbiol **54**:86–92

Breglia SA, Yubuki N, Hoppenrath M, Leander BS (2010) Ultrastructure and molecular phylogenetic position of a novel euglenozoan with extrusive episymbiotic bacteria: *Bihospites bacati* n. gen. et sp. (Symbiontida). BMC Microbiol **10**:145

Busse I, Preisfeld A (2003) Discovery of a group I intron in the SSU rDNA of *Ploeotia costata* (Euglenozoa). Protist **154**:57–69

Busse I, Patterson DJ, Preisfeld A (2003) Phylogeny of phagotrophic euglenids (Euglenozoa): A molecular approach based on culture material and environmental samples. J Phycol **39**:828–836

Capella-Gutiérrez S, Silla-Martínez JM, Gabaldón T (2009) trimAl: a tool for automated alignment trimming in large-scale phylogenetic analyses. Bioinformatics **25**:1972–1973

Cavalier-Smith T (2016) Higher classification and phylogeny of Euglenozoa. Europ J Protistol **56**:250–276

Cavalier-Smith T (2017) Euglenoid pellicle morphogenesis and evolution in light of comparative ultrastructure and trypanosomatid biology: Semi-conservative microtubule/strip duplication, strip shaping and transformation. Europ J Protistol **61**:137–179

Cavalier-Smith T, Chao EE, Vickerman K (2016) New phagotrophic euglenoid species (new genus *Decastava; Scytomonas saepesedens; Entosiphon oblongum*), Hsp90 introns, and putative euglenoid Hsp90 pre-mRNA insertional editing. Europ J Protistol **56**:147–170

Chan Y-F, Chiang K-P, Chang J, Moestrup Ø, Chung C-C (2015) Strains of the morphospecies *Ploeotia costata* (Euglenozoa) isolated from the western North Pacific (Taiwan) reveal substantial genetic differences. J Eukaryot Microbiol **62**:318–326

Chan Y-F, Moestrup Ø, Chang J (2013) On *Keelungia pulex* nov. gen. et nov. sp., a heterotrophic euglenoid flagellate that lacks pellicular plates (Euglenophyceae, Euglenida). Europ J Protistol **49**:15–31

Dietrich D, Arndt H (2000) Biomass partitioning of benthic microbes in a Baltic inlet: relationships between bacteria, algae, heterotrophic flagellates and ciliates. Mar Biol **136**:309–322

Dujardin F (1841) Histoire naturelle des Zoophytes: Infusoires. Librairie Encyclopédique de Roret, Paris, 684 p.

Esson HJ, Leander BS (2006) A model for the morphogenesis of strip reduction patterns in phototrophic euglenids: evidence for heterochrony in pellicle evolution. Evol Dev **8**:378–388

Esson HJ, Leander BS (2008) Novel pellicle surface patterns on *Euglena obtusa* (Euglenophyta) from the marine benthic environment: implications for pellicle development and evolution. J Phycol **44**:132–141

Ekebom J, Patterson DJ, Vørs N (1995) Heterotrophic flagellates from coral reef sediments (Great Barrier Reef, Australia). Arch Protistenkd **146**:251–272

Farmer MA, Triemer RE (1988) A redescription of the genus *Ploeotia* Duj. (Euglenophyceae). Taxon **37**:319–325

Farmer MA, Triemer RE (1994) An ultrastructural study of *Lentomonas applanatum* (Preisig) N. G. (Euglenida). J Eukaryot Microbiol **41**:112–119

Gawryluk RMR, del Campo J, Okamoto N, Strassert JFH, Lukeš J, Richards TA, Worden AZ, Santoro AE, Keeling PJ (2016) Morphological identification and single-cell genomics of marine diplonemids. Curr Biol **26**:3053–3059

Goddard MR, Burt A (1999) Recurrent invasion and extinction of a selfish gene. Proc Natl Acad Sci USA **96**:13880–13885

Gouy M, Guindon S, Gascuel O (2010) SeaView Version 4: a multiplatform graphical user interface for sequence alignment and phylogenetic tree building. Mol Biol Evol **27**:221–224

Gumińska N, Płecha M, Zakryś B, Milanowski R (2018) Order of removal of conventional and nonconventional introns from nuclear transcripts of *Euglena gracilis*. PLoS Genet **14**, e1007761–16

Haugen P, Simon DM, Bhattacharya D (2005) The natural history of group I introns. Trends Genet **21**:111–119

Henze K, Badr A, Wettern M, Cerff R, Martin W (1995) A nuclear gene of eubacterial origin in *Euglena gracilis* reflects cryptic endosymbioses during protist evolution. Proc Natl Acad Sci USA **92**:9122–9126

Jackson C, Knoll AH, Chan CX, Verbruggen H (2018) Plastid phylogenomics with broad taxon sampling further elucidates the distinct evolutionary origins and timing of secondary green plastids. Nat Ecol Evol **8**:1–10

Karnkowska A, Bennett MS, Watza D, Kim JI, Zakryś B, Triemer RE (2015) Phylogenetic relationships and morphological character evolution of photosynthetic euglenids (Excavata) inferred from taxon-rich analyses of five genes. J Eukaryot Microbiol **62**:362–373

Katoh K, Standley DM (2013) MAFFT multiple sequence alignment software version 7: improvements in performance and usability. Mol Biol Evol **30**:772–780

Kearse M, Moir R, Wilson A, Stones-Havas S, Cheung M, Sturrock S, Buxton S, Cooper A, Markowitz S, Duran C, Thierer T, Ashton B, Meintjes P, Drummond A (2012) Geneious Basic: an integrated and extendable desktop software platform for the organization and analysis of sequence data. Bioinformatics **28**:1647–1649

Kim E, Park JS, Simpson AGB, Matsunaga S, Watanabe M, Murakami A, Sommerfeld K, Onodera NT, Archibald JM (2010) Complex array of endobionts in *Petalomonas sphagnophila*, a large heterotrophic euglenid protist from *Sphagnum*-dominated peatlands. ISME J **4**:1108–1120

Kolisko M, Boscaro V, Burki F, Lynn DH, Keeling PJ (2014) Single-cell transcriptomics for microbial eukaryotes. Curr Biol **24**:R1081–R1082

Larsen J (1987) Algal studies of the Danish Wadden Sea. IV. A taxonomic study of the interstitial euglenoid flagellates. Nord J Bot **7**:589–607

Larsen J, Patterson DJ (1990) Some flagellates (Protista) from tropical marine sediments. J Nat Hist **24**:801–937

Larsson A (2014) AliView: a fast and lightweight alignment viewer and editor for large datasets. Bioinformatics **30**:3276–3278

Lax G, Simpson AGB (2013) Combining molecular data with classical morphology for uncultured phagotrophic euglenids (Excavata): A single-cell approach. J Eukaryot Microbiol **60**:615–625

Lax G, Eglit Y, Eme L, Bertrand EM, Roger AJ, Simpson AGB (2018) Hemimastigophora is a novel supra-kingdom-level lineage of eukaryotes. Nature **564**:410–414

Leander BS (2004) Did trypanosomatid parasites have photosynthetic ancestors? Trends Microbiol **12**:251–258

Leander BS, Farmer MA (2001) Comparative morphology of the euglenid pellicle. II. Diversity of strip substructure. J Eukaryot Microbiol **48**:202–217

Leander BS, Esson HJ, Breglia SA (2007) Macroevolution of complex cytoskeletal systems in euglenids. Bioessays **29**:987–1000

Leander BS, Triemer RE, Farmer MA (2001a) Character evolution in heterotrophic euglenids. Eur J Protistol **37**:337–356

Leander BS, Witek RP, Farmer MA (2001b) Trends in the evolution of the euglenid pellicle. Evolution **55**:2215–2235

Leander BS, Lax G, Karnkowska A, Simpson AGB (2017) Euglenida. In Archibald JM, Slamovits CH, Simpson AGB (eds) Handbook of the Protists. Springer International Publishing, Cham, pp 1047–1088

Lee WJ (2008) Free-living heterotrophic euglenids from marine sediments of the Gippsland Basin, southeastern Australia. Mar Biol Res **4**:333–349

Lee WJ (2012) Free-living benthic heterotrophic euglenids from Botany Bay, Australia. Mar Biol Res **8**:3–27

Lee WJ, Patterson DJ (2000) Heterotrophic flagellates (Protista) from marine sediments of Botany Bay, Australia. J Nat Hist **34**:483–562

Lee WJ, Patterson DJ (2002) Abundance and biomass of heterotrophic flagellates, and factors controlling their abundance and distribution in sediments of Botany Bay. Microb Ecol **43**:467–481

Lee WJ, Simpson AGB (2014a) Ultrastructure and molecular phylogenetic position of *Neometanema parovale* sp. nov. (*Neometanema* gen. nov.), a marine phagotrophic euglenid with skidding motility. Protist **165**:452–472

Lee WJ, Simpson AGB (2014b) Morphological and molecular characterisation of *Notosolenus urceolatus* Larsen and Patterson 1990, a member of an understudied deep-branching euglenid group (petalomonads). J Eukaryot Microbiol **61**:463–479

Lee WJ, Simpson AGB, Patterson DJ (2005) Free-living heterotrophic flagellates from freshwater sites in Tasmania (Australia), a field survey. Acta Protozool **44**:321–350

Linton EW, Triemer RE (1999) Reconstruction of the feeding apparatus in *Ploeotia costata* (Euglenophyta) and its relationship to other euglenoid feeding apparatuses. J Phycol **35**:313–324

Milanowski R, Karnkowska A, Ishikawa T, Zakryś B (2014) Distribution of conventional and nonconventional introns in tubulin (α*and*β) genes of euglenids. Mol Biol Evol **31**:584–593

Montegut-Felkner AE, Triemer RE (1997) Phylogenetic relationships of selected euglenoid genera based on morphological and molecular data. J Phycol **33**:512–519

Paerschke S, Vollmer AH, Preisfeld A (2017) Ultrastructural and immunocytochemical investigation of paramylon combined with new 18S rDNA-based secondary structure analysis clarifies phylogenetic affiliation of *Entosiphon sulcatum* (Euglenida: Euglenozoa). Org Divers Evol **59**:1–12

Patterson DJ, Simpson AGB (1996) Heterotrophic flagellates from coastal marine and hypersaline sediments in Western Australia. Europ J Protistol **32**:423–448

Picelli S, Björklund ÅK, Faridani OR, Sagasser S, Winberg G, Sandberg R (2013) Smart-seq2 for sensitive full-length transcriptome profiling in single cells. Nat Methods **10**:1096–1098

Ronquist F, Teslenko M, van der Mark P, Ayres DL, Darling A, Höhna S, Larget B, Liu L, Suchard MA, Huelsenbeck JP (2012) MrBayes 3. 2: Efficient Bayesian phylogenetic inference and model choice across a large model space. Syst Biol **61**:539–542

Schroeckh S, Lee WJ, Patterson DJ (2003) Free-living heterotrophic euglenids from freshwater sites in mainland Australia. Hydrobiologia **493**:131–166

Stamatakis A (2014) RAxML version 8: a tool for phylogenetic analysis and post-analysis of large phylogenies. Bioinformatics **30**:1312–1313

Triemer RE (1986) Light and electron microscopic description of a colorless euglenoid *Serpenomonas costata* n. g., n. sp. J Protozool **33**:412–415

Triemer RE, Fritz L (1987) Structure and operation of the feeding apparatus in a colorless euglenoid, *Entosiphon sulcatum*. J Protozool **34**:39–47

Triemer RE, Fritz L (1988) Ultrastructural features of mitosis in *Ploeotia costata* (Heteronematales, Euglenophyta). J Phycol **24**:514–519

Turmel M, Gagnon M-C, O'Kelly CJ, Otis C, Lemieux C (2008) The chloroplast genomes of the green algae *Pyramimonas, Monomastix,* and *Pycnococcus* shed new light on the evolutionary history of prasinophytes and the origin of the secondary chloroplasts of euglenids. Mol Biol Evol **26**:631–648

von der Heyden S, Chao EE, Vickerman K, Cavalier-Smith T (2004) Ribosomal RNA phylogeny of bodonid and diplonemid flagellates and the evolution of Euglenozoa. J Eukaryot Microbiol **51**:402–416

Yubuki N, Simpson AGB, Leander BS (2013) Reconstruction of the feeding apparatus in *Postgaardi mariagerensis* provides evidence for character evolution within the Symbiontida (Euglenozoa). Europ J Protistol **49**:32–39

Zhou Y, Lu C, Wu Q-J, Wang Y, Sun Z-T, Deng J-C, Zhang Y (2007) GISSD: Group I Intron sequence and structure database. Nucleic Acids Res **36**:D31–D37